DOT/FAA/TC-21/37

Federal Aviation Administration
William J. Hughes Technical Center
Aviation Research Division
Atlantic City International Airport
New Jersey 08405

Minimizing Risk of Bird Strike to Rotorcraft

November 3, 2021

Final report

U.S. Department of Transportation
Federal Aviation Administration

NOTICE

This document is disseminated under the sponsorship of the U.S. Department of Transportation in the interest of information exchange. The U.S. Government assumes no liability for the contents or use thereof. The U.S. Government does not endorse products or manufacturers. Trade or manufacturers' names appear herein solely because they are considered essential to the objective of this report. The findings and conclusions in this report are those of the author(s) and do not necessarily represent the views of the funding agency. This document does not constitute FAA policy. Consult the FAA sponsoring organization listed on the Technical Documentation page as to its use.

This report is available at the Federal Aviation Administration William J. Hughes Technical Center's Full-Text Technical Reports page: actlibrary.tc.faa.gov in Adobe Acrobat portable document format (PDF).

Technical Report Documentation Page

Form DOT F 1700.7 (8-72) Reproduction of completed page authorized

1. Report No.	2. Government Accession No.	3. Recipient's Catalog No.
DOT/FAA/TC-21/37		

4. Title and Subtitle	5. Report Date
Minimizing Risk of Bird Strike to Rotorcraft	Month Year
	6. Performing Organization Code

7. Author(s)	8. Performing Organization Report No.
Donald J. Ronning	

9. Performing Organization Name and Address	10. Work Unit No. (TRAIS)
Lite Enterprises 4 Bud Way, Suite 15 Nashua, NH 03063-1740	11. Contract or Grant No.

12. Sponsoring Agency Name and Address	13. Type of Report and Period Covered
FAA William J. Hughes Technical Center Building 300, Fourth Floor Atlantic City International Airport Atlantic City NJ 08405	Final Report
	14. Sponsoring Agency Code

15. Supplementary Notes

The FAA William J. Hughes Technical Center Aviation Research Division COR/Tech. Rep was Daniel P. Dellmyer.

16. Abstract

This research presents a set of investigation results of a prototype (PAR46 size) landing light that incorporated ultraviolet light emitting diodes (UVLEDs) in 'real-world' flight conditions for the benefit of Bird Strike Mitigation for Rotorcraft.

The research measured the effectiveness of using a prototype Bird UVLEDs integrated into a PAR46 landing light to trigger bird avoidance behavioral responses, which would increase flight path separation to reduce the incidence of bird strikes. The first set of field trials involved a one-quarter scale remote controlled (RC) plane. The second set of field trials involved an AirTractor 802 aircraft performing flight operations, with nominal flight speeds of 150 kt and < 100' above ground level (AGL), in the performance of agricultural chemical delivery.

Concrete examples are illustrated throughout the report to make the concepts clear. Field data of measured bird responses to the deterrence device ON/OFF condition of the PAR46 with UVLED landing light was statistically modeled for correlation with environmental conditions. The environmental flight conditions were recalculated to determine the SNR (signal to noise ratio) of the bird's visual system to the approaching plane, corresponding to the time of change in bird behavior identified as flight direction, altitude, or speed as recorded by an on-board video camera. The camera was mounted in the cockpit of an AirTractor air vehicle with a majority of plane-bird interactions occurring at 3-10m AGL with an airspeed of 150 kt. The three empirically derived variables ($V1$, $V2$, and $V3$) of the model correspond to three sequential steps involved in visual processing as presented by modern neurophysiological research. The SNR of the air vehicle to the background brightness of the sky is a key factor incorporated in the model that differentiates the predicted distance of the birds' distance of change in flight direction, altitude, or speed. Multiple species of birds were involved in these field trials, which benefited from the ON condition of the prototype (PAR46 size) landing light that incorporated UVLEDs. Differences of reaction distance were measured for various species, which may be uniquely associated with the species neurophysiological functions.

17. Key Words	18. Distribution Statement
Bird strike, Airspace separation, ultraviolet, PAR46	This document is available to the U.S. public through the National Technical Information Service (NTIS), Springfield, Virginia 22161. This document is also available from the Federal Aviation Administration William J. Hughes Technical Center at actlibrary.tc.faa.gov.

19. Security Classif. (of this report)	20. Security Classif. (of this page)	21. No. of Pages	22. Price
Unclassified	Unclassified	44	

Acknowledgements

Dr. Nancy Dirubbo for valuable advice on the experimental design and for useful comments on the manuscript, DeTect Inc. for providing the bird detection radar system used in this study and assistance in interpretation of the data, and Whirlwind Aviation (FAA Identifier 48AR) for supporting the ¼-scale model aircraft and the full-scale air vehicle flight operations of the field trials. We also thank the following people who worked tirelessly to provide the operational support required to execute these field trials: Donald Ducharme, Elizabeth Keefe, David Newberry, and Chrissy and Rodney Shelley. Results were published and subsequent copyrights remain with *SAE Int. J. Aerosp.* [12(2):99.-116,2019] and subsequent publication.

Contents

Figures

Tables

Acronyms

Acronym	Definition
AGL	Above ground level
ATC	Air traffic control
FAA	Federal Aviation Administration
LED	Light-emitting diode
LiPo	Lithium polymer battery
RC	remote controlled
SNR	signal-to-noise ratio
UVLEDs	ultraviolet light emitting diodes
WHA	Wildlife Hazard Assessments
WHMP	Wildlife Hazard Management Plan

Executive summary

Current methods of bird strike mitigation need to be improved to reduce both human and avian morbidity, mortality and financial losses for rotorcraft, as well as all air vehicles. After considering current mitigation techniques and their theoretical basis, and reviewing the literature of the most recent research of avian neuropathophysiology, a novel approach using ultraviolet light emitting diodes (***UVLEDs***) in landing lights was developed with the goal to further reduce bird strikes.

This research measured the effectiveness of using a prototype ***PAR46*** landing light with ***UVLEDs*** (***PAR46$_{UVLED}$***) to effect a bird avoidance behavioral response that would increase flight path separation thereby reducing the incidence of bird strikes. The first set of field trials involved a ¼-scale remote controlled (***RC***) plane. The second set involved an AirTractor 802 aircraft, flying at nominal speeds (150 kt) and < 100' above ground level (***AGL***), in the performance of agricultural chemical delivery.

Field data of measurements of bird responses to the deterrence device ***ON*** vs ***OFF*** condition were statistically modeled for correlation with environmental conditions. The signal to noise ratio (***SNR***) of the bird's visual system to the approaching plane was calculated. The three sequential steps (***V1***, *V2*, and ***V***3) of a visual processing model was developed based upon modern avian neurophysiological research to provide a predicted distance to the plane-bird interactions.

This study demonstrated increased flight path separation between all bird species and air vehicles with ***PAR46$_{UVLED}$*** landing light turned ***ON*** vs ***OFF***, as measured in the field tests. The results of this 'real-world' field study measured the behavioral responses for different avian species that the avian visual perception model predicted. The results are supportive of the modern visual processing model involving three sequential steps representing visual capture, retinal neural coding response, and the brain's sensing complex nonlinear neural response. Further investigation in the underlying complexities of the Optical–Visual–Cognitive Theories offers new insights to reducing the risks of bird strikes.

The results demonstrated increased flight path separation between birds and air vehicles with ***PAR46$_{UVLED}$*** were statistically significant. The increased bird's awareness and quicker behavioral response to the approaching air vehicle offers a reduction of the risk of a bird strike. The prototype landing light is designed to be readily installed and operated in any air vehicle without requiring modifications or adding to the pilot's workload. The operation of the ***PAR46$_{UVLED}$*** landing light is at the discretion of the pilot.

1 Introduction

This research was undertaken in response to DTFACT-16-R-00021, AAQ-610 Facilities & Grants, solicitation posted by the Federal Aviation Administration William J. Hughes Technical Center. The goal of this task was to research Bird Strike Mitigation Processes for Rotorcraft.

1.1 Purpose

This research was structured to measure the reaction of flying birds to approaching air vehicles fitted with a fully functional ***PAR46*** landing light that incorporated ***UVLEDs.*** The field tests were conducted in northeastern rural Arkansas where flooded rice and irrigated soybean fields are found. The test site chosen was the airfield (FAA Identifier 48AR) owned and operated by an agricultural pilot located east of Fisher, Arkansas, USA (35°29′17.0″N 90°50′28.3″W) (see Figure 1).

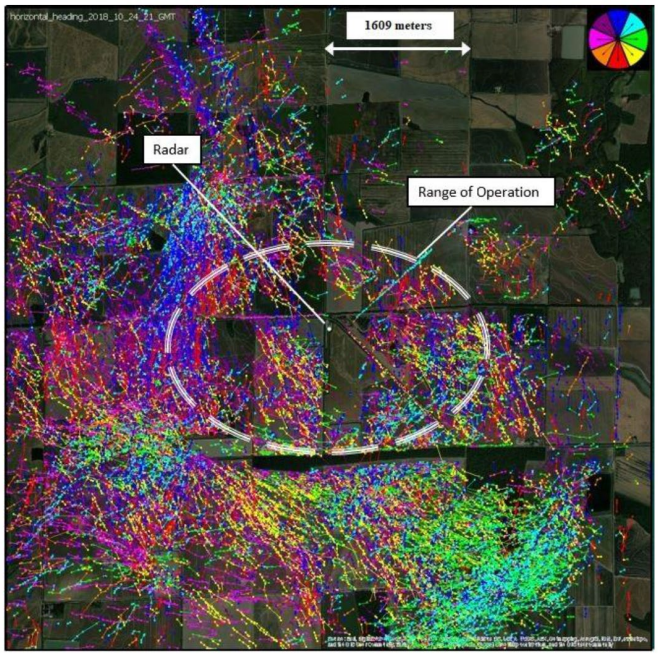

Figure 1. Radar, airfield, and range limit of flight operations from radar unit for first field test. The birds' tracks are color coded to show flight direction.

The first field test utilized a ¼-scale remote-controlled (***RC***) plane flown in a straight, level altitude and constant airspeed with an intersecting flight path between the aircraft and birds at approximately the same altitude. All flight operations for both field trials were conducted during daylight hours. The birds were exposed to the illumination of a single $\boldsymbol{PAR46_{UVLED}}$ landing light mounted on a ***RC*** aircraft, which were both remotely controlled from the ground. The ***RC*** plane

was flown in the direction of flocks of geese and ducks throughout the month of November 2018. The behavioral effect of birds interacting with an ***RC*** aircraft in flight was recorded by radar, cameras, and multiple human observers. Flight duration with the ¼-scale model airplane was limited to 15 minutes due to the capacity of onboard fuel, limiting operations to one-mile distance from the pilot's location on the airfield.

The second field test, which utilized an AirTractor 802 air vehicle, was performed within 60 km of the airfield at nominal flight speed of 150 kt and <100' ***AGL*** (77 m/s @ 3-10 m ***AGL*** typical) in the performance of agricultural chemical delivery. This involved straight and level flights during delivery of chemicals as it traversed the agricultural fields during the months of January through April 2021.

1.2 Background

This document presents results from two separate field studies to understand 'real world' bird behavior to an approaching air vehicle configured with $\boldsymbol{PAR46_{UVLED}}$ landing light(s) that were either ***ON*** or ***OFF***. The derived model was developed using widely accepted laws of optics and engineering in conjunction with the most recent postulates of avian neurophysiology.

The risk, frequency, and potential severity of wildlife-aircraft collisions are expected to grow over the next decade based on increasing air traffic, growing bird populations, and the increased use of aircraft with fewer engines. The annual cost of wildlife strikes is projected to be a minimum of $142 million in the USA, and some estimates list it at twice this number [1]. This includes a minimum of 71,253 hours of aircraft downtime for the aviation industry [1]. Aviation bird strikes effect many stakeholders, including pilots, mechanics, airlines, airport operators, air traffic controllers, wildlife personnel, aviation safety analysts, airplane and engine manufacturers, flight training organizations, military operations, and the traveling public.

The reported incidence of aircraft bird strikes to both rotorcraft and fixed-wing aircraft is increasing despite current wildlife mitigation techniques [2]. This study explores a novel approach to reducing bird strikes and does not conform to prior aviation study models, which to date have not found an effective midair mitigation system. Bird strikes to rotorcraft and fixed-wing aircraft pose a major threat, and more effective techniques are needed to mitigate these bird strikes [1]. A total of 1,758 rotorcraft bird strikes were recorded between 1990 and March 2016, of which 582 (33%) damaged the rotorcraft. The species of the bird strike was identified only 37% of the time [3]. The number of bird strikes occurring during the day was 54%, 42% at night, and 4% during dusk/dawn hours [3]. The FAA Wildlife Database shows that 69% of the reported rotorcraft bird strikes occurred during the en route phase of flight. Rotorcraft typically cruise at

altitudes between 150 and 1,500 m and are exposed to a greater bird strike risk than fixed-wing aircraft that cruise at altitudes of approximately 11,000 m [3].

The Fact Sheet, the Federal Aviation Administration's (FAA) Wildlife Hazard Mitigation Program, reports that in the decades from 1988 to 2018, wildlife strikes have killed more than 287 people and destroyed over 263 aircraft globally [3]. Birds were involved in 95% of those strikes [1]. The number of reported strikes increased from 2000 to 2017 by 144% in the USA, while the number of damaging strikes declined 16% [1]. Bird strike reporting has increased 7.4 times from 1,850 in 1990 to over 13,000 for the last four years 2014-2017 (14,496 in 2017) [1]. The FAA mandated strike reporting for air traffic control (ATC) personnel (ATO Order JO 7210.632: January 30, 2012) and established an outreach effort to increase awareness several years ago, which contributed to a general increase in reporting. Airport management has a duty under FAR Part 139 to mitigate wildlife hazards on the airport. ATC has a duty under FAA Order 7110.65, paragraph 2-1-22, to inform other pilots, other ATC facilities, and automated flight service stations about the hazard. The gradual decrease in 5% of reported strikes as damaging strikes is attributed to the general increase in reporting of all strikes, and numerous design and ruggedness improvements by aircraft manufacturers.

Bird strikes at or near airports during takeoff or landing account for about 90% of the total number of reported bird strikes involving civil aircraft [1]. The FAA requires airport sponsors to conduct Wildlife Hazard Assessments (WHA) and prepare Wildlife Hazard Management Plans (WHMPs) to mitigate wildlife hazards through habitat modification, harassment technology, and research [4]. While most bird strikes occur on the ground or at low altitude, they also occur in flight. This group of bird strikes is outside the range of airport centric control measures.

A review of the literature demonstrates three techniques currently employed to reduce bird strikes [5], as follows:

1. Aircraft engineering to reduce the damage of collision
2. The creation of airport bubbles to keep wildlife out of vulnerable flight areas
3. Flight path separation modalities to detect and modify flight paths of aircraft or birds

A technique that enables increased flight path separation by inducing an earlier response by the birds would offer an opportunity to further reduce bird strikes both at airports and during en route flight operations. This technique would be beneficial in a variety of high-risk environments, such as low altitude and high speeds, and for flight operations in areas without the benefit of airfields using wildlife management practices [5].

Avian color research is patterned on human color models that do not account for the complexities of the neurophysiological and cognitive mechanisms involved in avian vision and object recognition [6, 7]. Several recent studies of the avian anatomy and neurophysiology responsible for visual perception contribute to a theoretical basis for mitigating bird strikes through visual sensory input [8, 9, 10, 11, 12, 13]. The results of this 'real-world' field study is highly correlated with a new understanding of avian visual perception and behavioral response patterned upon the modern-day neurological studies, which static tetra-color chromatic contrasts models struggle to describe.

The concepts of sensory perception and cognitive recognition leading to action have been long studied. A cognitive process may involve various forms: attention, thought, learning, etc. The theoretical question on the structural mechanism of visual sensing, and the relation between visual perception and cognition theories, has remained an unresolved debate since Newton discovered in 1665 (and published in 1674 and 1704) that sunlight passing through a prism separates into multiple colors could be recombined to make the light white again. Numerous theories and models have been proposed and intensely debated, starting with 'The Helmholtz-Hering Debate' (see Figure 2), leading to the modern-day debate by psychologists as to the nature of visual perception. The Gibson's hypothesis (1966) bottom up theory suggests that perception involves innate mechanisms forged by evolution and that no learning is required, with each successive stage in the visual pathway carrying out ever more complex analysis [14]. Gregory's theory (1970), known as the top-down processing model, proposes that contextual information based on past experiences and stored memory patterns, is interpreted like pattern recognition (see Figure 3). The most recent avian visual research suggests sequential processing involves direct and indirect neural pathways performing complex linear, nonlinear, algebraic, and differential signal processing involving directionally sensitive neurons [8, 12, 15, 16]. A typical retinal ganglion cell presents a center region with either excitation or inhibition and a surround region with the opposite sign and bounded by the resolving power and the lateral inhibition. The retinal ganglion cell structure varies from species to species. However, the underlying biological and neurological interactions are similar.

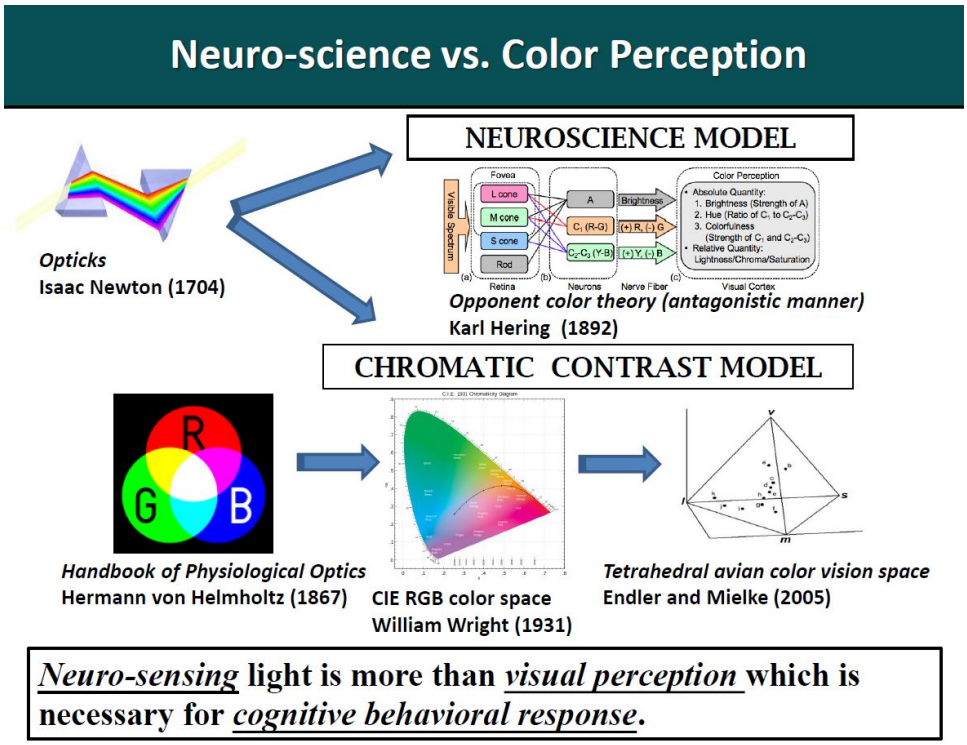

Figure 2. Divergence of Neuro-science vs Color Perception Theories

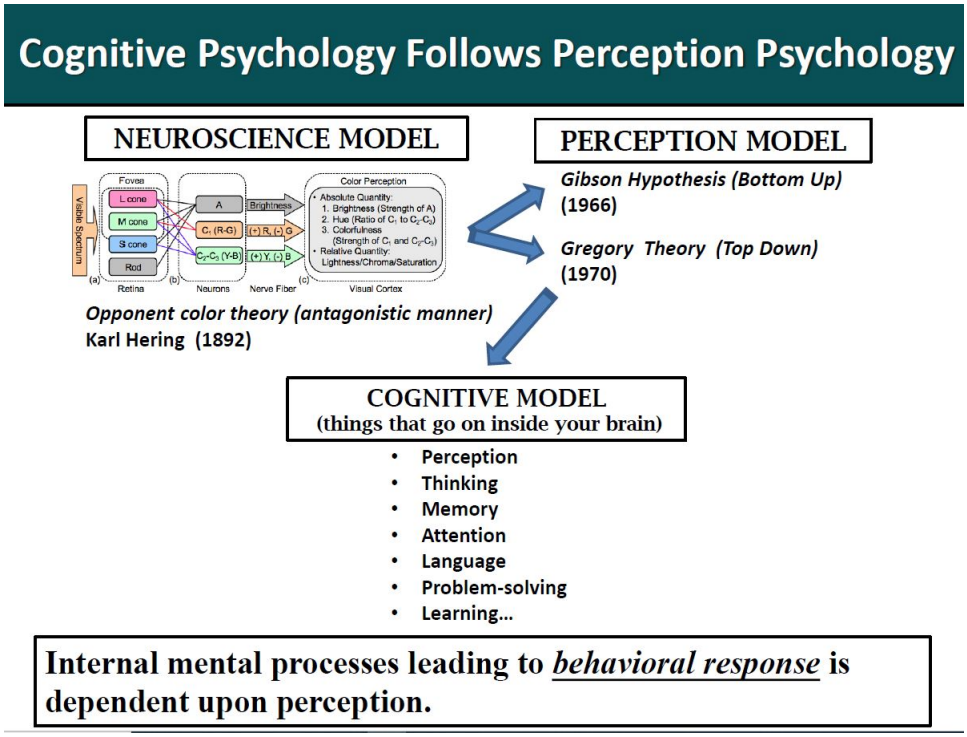

Figure 3. Divergence of Optical–Visual–Cognitive Theories

Birds commonly have tetrachromatic color sensitivity seeing red, green, blue, and ultraviolent spectral ranges in combination with rods, whereas humans have rods and trichromatic vision with retinal cone receptors for red, green, and blue only [9, 17]. Studies demonstrate that avian visual systems can vary within species [12, 13, 15, 16, 17, 18, 19, 20, 21]. Pulsing light is known to induce pupil dilation and improve motion perception [22]. The presence of UV wavelengths improves the temporal resolution of the avian visual system [17] and reduces Sandhill Crane collisions with power lines [22]. Recent research efforts to relate chromatic contrast theories are being extrapolated to describe behavioral responses within the predator-prey framework and studied the shape of drones as a frightening device [23]. More research needs to be done to validate these theories to increase our understanding of avian behavioral responses.

The avoidance of an imminent encounter between a bird and air vehicle requires an awareness of the risk of an impending collision for the bird(s), the aircraft, or both. Increasing the distance at which awareness of an impending convergence of flight paths occurs increases the time available to react, thereby decreasing the risk of collision. This study follows the new understanding of the complex biological mechanisms of avian vision [10, 13, 15, 16, 20, 21]. A range of avian behaviors involving self-control, working memory, and cognitive flexibility have been studied within an evolutionary framework. Comparative avian studies have identified differences in avian brain structures [20]. Species-specific electrical pathways processing visual color information have been identified. The early impulse of the birds' visual sensors triggers the transmission signal to the brain enabling an awareness and a behavioral response to that signal. The behavioral response may vary by the individual bird or within a flock's behavioral pattern. This understanding led to the development of the prototype landing light. The goal of the research was to measure the difference of plane-bird midair interactions with random flocks of varying sizes of varying avian species in their natural (wild) environment when illuminated by ***PAR46$_{UVLED}$***.

Figure 4 shows the prototype ***PAR46$_{UVLED}$*** landing light mounted in a workbench test fixture. Note that the operation of the UVLEDs does not interfere with the white landing light function, which produces 20.78 W of emitted power per set of UVLEDs. The 420 nm LEDs were switched at a rate greater than 30 hertz (Hz) while the 395 nm and 375 nm LEDs are alternatively switched at a rate less than 2 Hz. The ***PAR46$_{UVLED}$*** sequentially pulsed the three UVLEDs, while the white LEDs were continuously turned ON when the ***PAR46$_{UVLED}$*** was powered. The custom fabricated electronic circuit of the landing light incorporates multiple LED drivers for four types of LEDs: white color, mono-color 420 nanometer (nm), mono-color 395 nm, and mono-color 375 nm. The near-UV wavelengths selected are well matched to the known peak sensitivity wavelengths of avian short wavelength cones [17]. A microcontroller unit independently

managed power to each of the LEDs. The white LEDs were continuously ***ON***, while each color set of UVLEDs were alternatingly pulsed to produce a repeating pattern of flash output. Each color set of UVLEDs was powered with 22.2 VDC at 1.8 A (39.96 W). The LED power conversion efficiency is 52%. The measured constant luminance of the fabricated ***PAR46$_{UVLED}$*** landing light was greater than 300 lux (***k***1) at 9.1 m (***k***2) from the surface of the light. The measurement distance of 9.1 m was required to prevent the landing light from saturating the probe and to avoid the near-field light propagation effects of the landing light.

Figure 4. Prototype ***PAR46$_{UVLED}$*** landing light operating in a test fixture

The **P*AR46$_{UVLED}$*** had a circular field of illumination of ±15°. The 28 V direct current (VDC) with 6.2 amperes (Amps) current supplied by the lithium polymer (LiPo) batteries fulfilled the power requirements during flight operations with the ¼-scale model airplane. The AirTractor 802 landing light electrical circuit powered and controlled the pair of ***PAR46$_{UVLED}$*** as a constant ***ON*** or ***OFF*** light (no 'wing-wag' blinking).

The first field trial involved the use of a ¼-scale ***RC*** airplane at reduced air speeds, while the second field trial involved a full-sized air vehicle performing flight operations at nominal 150 kt air speed. Both field studies followed nominal straight and level flight profiles. The first field trial exclusively involved mid-air plane-bird interactions. The second field trial involved a mix of mid-air as well as ground-air plane-bird interactions with a flying air vehicle.

Both field trials involved the collection of field-recorded data or calculated values for each plane-bird interaction (see Table 1).

Table 1. Field recorded and calculated values (plane-bird interaction)

DATA	**How recorded**
Date	Month, day, year
Time	GPS referenced
Temperature	Celsius
Wind speed	Meters per second
Wind direction	Compass points
Precipitation rate	Mist, moderate, heavy
Cloud cover	Clear, partly, overcast (Illuminance **[*I*]** Lux)
Birds species	Geese, ducks, mixed passerines
Bird number	Estimated flock size
Bird direction	Compass points
Bird speed	Meters per second
Birds altitude	Meters
Direction of diversion	Left, right, reversal, Mixed
Reaction energy expended **(*Epb*)**	None, mild, moderate, strong
Plane direction	Compass points
Plane speed *A*	Meters per second
Plane altitude	Meters
PAR46 with UVLEDs	ON, OFF (1, 0)
Plane-bird distance **(*Dpb*)**	Meters (radar, etc.)
Plane/bird intercept angle	Behind, side, head-on
Plane backlit by the sun	Behind, side, head-on
PAR46 irradiance @ plane bird distance **(*Ee*)**	Lux (calculated)
Signal-to-noise ratio **(*SNR*)**	Numerical ratio
Plane detection of eye **(*PD(eye)*)**	Figure of merit (calculated)

The illuminance (***I***) was measured by facing the probe of a HS1010 Illuminance Brightness Lux Meter/Light Meter manufactured by Bonajay (Shenzhen) Technology Co., Ltd., which is calibrated for CIE photo optic spectral response, in the opposite direction of the sun.

The three empirically derived variables (***V***1, ***V***2, and ***V***3), representing each sequential step involved in visual processing, were calculated for each field trial with the complete ***ON*** vs ***OFF*** dataset. The three high-level variables independently encompass several different models

(chromatic contrast, optical flow, predator-prey behavior, etc.) measured physiological and behavioral differences of species in a complimentary manner without bias. The comparison of the predicted distance of plane-bird interaction distance was correlated to the actual plane-bird distance separately for the both ***ON*** and ***OFF*** datasets. Further analysis of the data subset categorizing different bird species from the second field trial is presented.

The intensity factor (***FI***) is a premeasured constant value of the relative illuminance of different portions of the sky for each compass point compared to the referenced illuminance value (***I***) measured at the start of each flight operation. The brightness of the sky predictably changes between looking toward the sun or away from the sun. The ***FI*** constant values were revalidated periodically throughout the first field trial. The ***FI*** constant values were utilized for the second field trial without revalidating the values. The predetermined constant values (***FI***) were measured to represent the illuminance of the sky in the direction of the birds' flight path angle, recorded as follows:

- 1 = sun is behind the birds
- 1.25 = compass position ±45° either side
- 2.5 = compass position ±90° from behind ±45° either side
- 6.5 = compass position ±135° from behind ±45° either side
- 8 = directly facing the sun ±45° either side.

The plane-bird distance (***Dpb***) was measured from radar data or other field reference data to determine the flight distance of separation between birds and the plane's location. The relationship of the plane location in relation to the position of the sun from the perspective of the birds was determined using the recorded time of day and flight direction data. The sun's position was measured in ±45° groups from the angle of the sun to the vector direction between the plane's and birds' flight path recorded as 0 = behind birds ±45°, 1 = side angle ±90° from behind ±45°, or 2 = head on ±45°.

The plane-bird intercept angle is the relationship of the plane compared to the vector paths between the plane and the birds' flight path. The resulting angle was categorized as ±45° by comparing the vector directions between the plane's and birds' flight path recorded as 0 = behind birds ±45°, 1 = side angle ±90° from behind ±45°, or 2 = head on ±45°.

The power condition of the $\boldsymbol{PAR46_{UVLED}}$ was recorded as 0 = ***OFF*** and 1 = ***ON***.

The ***Ee*** is the irradiance from the $\boldsymbol{PAR46_{UVLED}}$ at the plane-bird distance (***Dpb***), as measured in lux (lumens/m2); $\boldsymbol{k}1$ and $\boldsymbol{k}2$ are empirically measured constants, and ***Dpb*** is determined from the radar and video images. The propagation of spatially and temporally incoherent light as a

function of [distance]$^{-2}$ as it moves through a homogeneous medium is derived from the field data.

$$\boldsymbol{Ee = k1 \times \left[\!\left[\frac{(k2)}{(Dpb)}\right]\!\right]^2} \quad (1)$$

PHeye is an empirically calculated number that generates an arbitrary value of postulated horizontal cell groups of the eye involved in the detection of the plane's wingspan at distance (***Dpb***). The calculated ratio of the known wingspan of the plane (***k***3) is divided by the product of the plane-bird distance multiplied by (***k***4). The (***k***4) value is a constant value equal to the tangent (θ) value of 0.5°. The rationale for $\theta = 0.5°$ is an arbitrarily defined small region of the retina corresponding to the interconnected horizontal cells. Note that the tangent value of small angles (less than 1°) will change approximately in a linear fashion.

$$\boldsymbol{PHeye = \frac{(k3)}{(Dpb)(k4)}} \quad (2)$$

The calculated signal-to-noise ratio (***SNR***) for each plane-bird interaction is a measure used in science and engineering that compares the level of a desired signal to the level of background noise. The equation for ***SNR*** is the ratio of the desired signal to the level of background signal (noise). The desired signal is the illuminance striking the bird's eye from the plane and $\boldsymbol{PAR46_{UVLED}}$ added to the background noise. The value of the background signal is defined as the illuminance of the sky in the direction of the birds' flight path measured by the illuminance flux measured at the start of each flight operation multiplied by the intensity factor (***FI***). It is the measure of irradiance of the light striking the bird's eye capable of causing various reactions such as pupillary dilation and accommodation reflex actions.

$$\boldsymbol{SNR = \frac{\big((Ee)x\ (PAR46\ ON\ or\ OFF)\big) + ((I)\ x\ (FI))}{(I)\ x\ (FI)}} \quad (3)$$

Three variables (***V***1, ***V***2, and ***V***3) are empirically derived values, which represent each sequential step involved in visual processing. The first variable (***V***1) is the value representing a bird's eye visual capture (i.e., optical system) for each plane-bird interaction equal to ***PHeye***. The second variable (***V***2) representing the retinal neural coding response to the bird's eye visual capture of the object by logarithmically adding the value ***PHeye*** with the signal strength defined as ***SNR*** (i.e., retinal neural processing) for each plane-bird interaction. The third variable (***V***3) is the value associated with the portion of the brain capable of sensing complex nonlinear neural response (i.e., changes in motion or patterns of an object) for each plane-bird interaction.

The linear regression analysis framework utilized variables (***V***1, ***V***2, and ***V***3) to the predicted distance of plane-bird interaction (***PDpb***) for each plane-bird interaction:

$$\boldsymbol{V1} = (\boldsymbol{PHeye}) \quad (4)$$

$$\boldsymbol{V2} = \boldsymbol{Log}\ \mathbf{10}\ (\boldsymbol{SNR}) + \boldsymbol{Log}\ \mathbf{10}\ (\boldsymbol{PHeye}) \quad (5)$$

$$\boldsymbol{V3} = (\boldsymbol{V2})(\boldsymbol{V2}) \quad (6)$$

These tests were used to analyze the dataset. Two tests, the Mann-Whitney and the two-sample Kolmogorov-Smirnov test from the XLSTAT-Premium software (Addinsoft, 2019; data analysis and statistics with MS Excel, Addinsoft, NY), were used. The nonparametric analysis techniques were applied to address the low conformance to a Gaussian distribution instead of a linear statistical analysis for the first field trial dataset only. Descriptive statistics and a regression method to model the three variables in a linear regression framework was obtained from the Excel Analysis ToolPak.

1.2.1 First field trial – experiment design

The bird radar unit was a 200 W, dopplerized capable S band frequency radar system, with 24° above ground level detection antenna configuration that performed a 360° sweep every 1.6 s with a corresponding vertical radar sweep (Merlin model manufactured by DeTect Inc., Panama City, FL) (see Figure 5). The Merlin model combines independent vertical and horizontal radar data to measure altitude. The radar unit did not record flight activities that were within that horizontal sweep cone of silence (see Figure 6). The radar tracks documented the location and altitude of the birds, and the flight behaviors of the flocks following the plane-bird interaction were recorded as (***Rpb***) intensity of bird response values. The camera mounted on the plane documented many avian behavioral responses not recorded by the radar. The temperature, wind direction, wind speed, and time were recorded by the airfield instrumentation (see Supplemental Material – spreadsheet) at the start of each flight operation.

The ¼ scale ***RC*** plane was a Valiant Model Hangar 9 design (Horizon Hobby LLC, Champaign, IL) with a color scheme consisting of a white background and red stripes. It has a 2.8 m wingspan with approximately 1.07 m2 wing surface area. The engine was a DLE 56RA gas engine with a tuned muffler system. The sound produced by this plane at full throttle was less than 96 dB at a distance of 6.1 m. A uniformly high throttle setting was utilized for all plane-bird interactions. All hardware and flight operations conformed to the Academy of Model

Aeronautics flight requirements. The additional payload consisted of the ***PAR46$_{UVLED}$***, a high-definition camera (110° field of view, 1920 x 1080 pixels, and 30 fps), lithium polymer (LiPo) batteries, controlling electronics, and relays to enable the ON/OFF operation. The ***PAR46$_{UVLED}$*** was mounted in the location where the cockpit windscreen would be located. The total weight of the additional payload was approximately 5 kg depending upon the capacity size of LiPo batteries used. Flight speed was generally limited to less than 21 m per second.

Figure 5. Bird detection radar location adjacent to the airstrip and hangar

Figure 6. Radar cone of silence as viewed from the cockpit

We found that the radar results were difficult to interpret when the field was overwhelmed with thousands of birds or multiple flocks traveling in dense groups in multiple directions. Some plane-bird interactions could not be corroborated with multiple record sets. Some of the flock reactions occurred beyond the view of the plane's camera, but they were seen by multiple human observers. Any bias in the collection or interpretation of the radar data is assumed to be equally applied to all data points collected.

1.2.2 Second field trial – experiment design

A single forward-facing GoPro 7 Black (1080p, 30 fps) camera mounted in the cockpit of the AirTractor 802 recorded the reactions of the birds. Interaction of birds that were within the direct

flight path of the air vehicle were recorded by the camera, which was configured with a field of view of approximately ±30°. The birds were exposed to the illumination from two ***PAR46$_{UVLED}$***, which were either ***ON*** or ***OFF*** condition throughout the entire flight operation. The maximum resolution of a single camera pixel corresponds to 0.26m at a distance of 1000m. Any bias in the collection or interpretation of the video is assumed to be equally applied to all data points collected. The temperature, wind direction, wind speed, and time were recorded by the airfield instrumentation (see Supplemental Material – spreadsheet) at the start of each flight operation.

1.2.3 First field trial – subjects

Large flocks of migrating snow geese (*Anser caerulescens*) and year-round resident greater white-fronted geese (*Anser albifrons*) were the dominant species in this study. Smaller groups of migrating Canada geese (*Branta canadensis*) and Ross's geese (*Anser rossii*) were present. Homogeneous flocks of migrating snow and Canada geese would overfly the aircraft at high altitudes, greater than 100 m. Flocks of mixed species found in the surrounding fields moved from one field to another to feed or to remote fields and nearby wildlife refuges. The number of dabbling ducks dramatically decreased in the nearby feeding fields when large flocks of geese were present. Therefore, they represented a smaller portion of the plane-bird interactions. These duck species included mallard (*Anas platyrhynchos*), northern pintail (*Anas acuta*), gadwall (*Mareca strepera*), blue-winged teal (*Spatula discors*), green-winged teal (*Anas carolinensis*), American wigeon (*Mareca americana*), and northern shoveler (*Spatula clypeata*). The study of the visual physiology of the Canada goose (*Branta canadensis*) has shown that they are capable of seeing objects between 324° and 340° horizontal field of view, have color streaks, and have UV cone peak sensitivity measured at 411 nm with a range exceeding 380-440 nm. It is hypothesized that the species involved in this study have similar physiology [9]. Large resident and migrating populations of geese and ducks were present. Often thousands of birds were flying in our immediate area of the airport with moments when tens of thousands of birds were flying at once (see Figure 7 and Figure 8).

Figure 7. The ¼-scale ***RC*** plane flown from the grass area adjacent to the airstrip

Figure 8. ***RC*** plane flown in the direction of large flocks of birds

1.2.4 Second field trial – subjects

The bird population of the second field test consisted of various resident populations, which were organized into general subsets: (*Anatidae*) geese & ducks, (*Icteridae*) + (*Quiscalus*) blackbirds & grackles, (*Ardeidae*) + (*Threskiornithidae*) Herons & Ibis, (*Accipitridae*) hawks & eagles, (*Corvidae*) crows & ravens, (*Charadriinae*) plover (*Passerine*) small body, and (*Cathartidae*) vulture species groups respectively. All unidentified species were categorized as an Unknown species group. The birds encountered were usually foraging in the fields or traversing between fields when the flight path of plane intersected with them.

1.2.5 First field trial – test and analysis procedure

Bird flight activity was the highest for several hours following sunrise or preceding sunset. The movement of cold weather fronts with predominately north winds brought large populations of migrating birds into our field of operation. We launched the ***RC*** plane for either high altitude migratory flocks at an altitude above 100 m as they were descending or local birds at lower altitude as they overflew our airspace. We interacted only with birds flying overhead and not

with birds located on the ground. All launches were from the airfield within 150 m of the radar unit located at the north end of the runway. The ***RC*** plane was operated in a manner to match the altitude of the birds and an intersecting approach flight path. The light was either continuously ***ON*** or ***OFF*** during each plane-bird interaction, which typically lasted less than 15 seconds and rarely more than 30 seconds. It was necessary to alter the plane's direction after a plane-bird interaction due to concerns of maintaining line-of-sight control and to ensure that the radio control limits were not exceeded. No predators were observed in the area during the conduct of the study.

Field data that corresponded to each plane-bird interaction were recorded. The radar measured both plane and bird speed and altitude. If either the birds or plane were not measured by the radar unit, video recording from the plane and the two additional cameras on the ground, combined with field notes, was used to estimate these values. All plane-bird interactions were traced to the global positioning system (GPS) time logged by the radar system.

1.2.6 Second field trial – test and analysis procedure

The unique avian family species involved in each bird-plane interaction (body size, shape, wingbeat pattern and/or flock pattern) was identified using the recorded images from the video camera. Most of the plane-bird interactions species were not identified and were assigned to an unknown group of species. The distance between the air vehicle and the bird was determined by multiplying the time difference recorded by camera between the moment of bird reaction to the approaching air vehicle and when it passed out of the field of view of the camera by the air speed of the air vehicle. The AirTractor's known $\boldsymbol{V_1}$, $\boldsymbol{V_r}$, $\boldsymbol{V_2}$, $\boldsymbol{V_n}$, and $\boldsymbol{V_{s1}}$ speeds corresponding to the flight condition at the time of bird-plane interactions were logged and utilized in calculating the airspace separation (distance) between the plane and the bird at the moment of reaction. The statistical treatment of the second field trial dataset follows the first field trial dataset.

1.2.7 First field trial – results

The mean distance of reaction of the ***PAR46$_{UVLED}$*** landing light ON was 334.7 m (n = 43) and OFF was 96.5 m (n = 32). The values for the UVLED ***ON*** ranged from 9.1 to 874.8 meters compared to values for the UVLED ***OFF*** recorded ranged from 9.1 to 676.7 m (see Table 2). The mean distance of reaction value for the lights ON is 3.5 times greater than the OFF value. The two-sample Kolmogorov-Smirnov test/two-tailed test determined that the distributions of the two datasets differ significantly (see Figure 9 and Figure 10) and are not equal (D = 0.674; p-value (two tailed), $p < 0.0001$). The instantaneous reaction of the birds, as recorded by either the plane's camera or from the two ground-based cameras, was noted.

Table 2. Descriptive statistics of the distance of response (meters) plane/birds (D_{pb})

Value	PAR46$_{UVLED}$ *OFF*	PAR46$_{UVLED}$ *ON*
Mean (meter)	96.46875	334.7121
Standard Error	22.50258	31.71274
Median	61	292.6
Mode	15.2	91.4
Standard deviation	127.2938	207.9544
Sample Variance	16203.71	43245.02
Kurtosis	15.2938	0.285569
Skewness	3.565886	0.837063
Range	676.7	874.82
Minimum	9.1	9.1
Maximum	685.8	883.92
Sum	3087	14392.62
Count	32	43
Confidence level (99.0%)	61.74801	85.56307

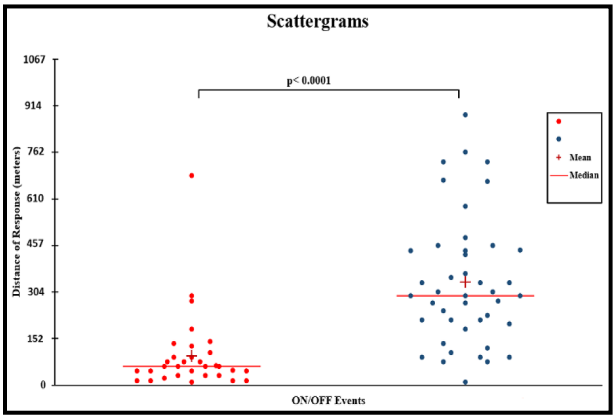

Figure 9. Scattergram illustrating birds' reaction distance to plane with ***PAR46$_{UVLED}$*** for ***ON*** vs ***OFF***

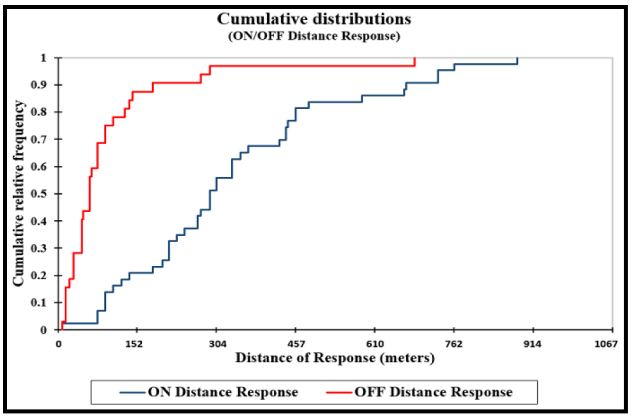

Figure 10. Cumulative population distribution with ***PAR46$_{UVLED}$ ON*** vs ***OFF***

1.2.8 Second field trial – results

The mean distance of reaction of the ***PAR46$_{UVLED}$*** landing light ON was 152.67 m (n = 170) and ***OFF*** was 99.83 m (n = 59). The values for ***ON*** ranged from 17 to 1334 meters. The values for the ***OFF*** recorded ranged from 25.5 to 296 m (see Table 3). The mean distance of reaction value for the lights ***ON*** is 1.5 times greater than the ***OFF*** value.

Table 3. Descriptive statistics of the distance of response (meters) plane/birds (D_{pb})

Value	PAR46$_{UVLED}$ ***ON***	PAR46$_{UVLED}$ ***OFF***
Mean (meter)	152.6700588	99.8338983
Standard Error	11.411	7.988
Median	119.8	78.3
Standard deviation	127.2938	207.9544
Sample Variance	16203.71	43245.02
Range	1317.000	270.500
Minimum	17.000	25.500
Maximum	1334.000	296.000
Sum	25953.910	5890.200
Count	170	59
Upper bound on mean (95%)	175.197	115.824
Upper bound on mean (95%)	175.197	115.824

The Two-sample t-test and z-test determined that the distributions of the two datasets is significantly different (see Figure 11) and are not equal (p-value (two tailed), $p < 0.0001$).

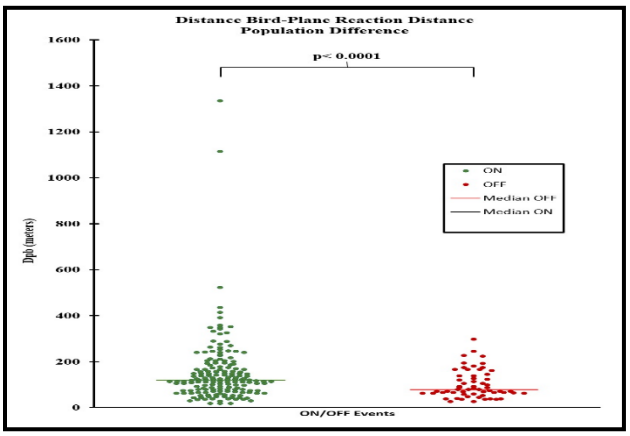

Figure 11. Scattergram of birds' reaction distance to plane with ***PAR46$_{UVLED}$ ON*** vs ***OFF***

The plot of cumulative distribution illustrates the total difference for the birds' reaction distance to the plane with ***PAR46$_{UVLED}$*** for the ***ON*** vs ***OFF*** conditions for plover (*Charadriinae),* herons (*Ardeidae)*, Ibis (*Threskiornithidae*), hawks (*Accipitridae*), eagles (large birds of prey of the family (*Accipitridae)*, vultures (*Cathartidae*), blackbirds (*Icteridae*), and grackles (*Quiscalus*), with a limited number of unidentified small-body (*Passerine*), waterfowl (*Anatidae*) species interactions. All unidentified species events were identified as an unknown group. Figure 12 shows the distribution for the birds' reaction distance to the plane with ***PAR46$_{UVLED}$*** for the ***ON*** vs ***OFF*** conditions for data subset of birds above or below 10 meters ***AGL***, and are similar while the combined data are different. Figure 13 shows the distribution of the birds' reaction distance to the plane, with ***PAR46$_{UVLED}$*** for the ***ON*** vs ***OFF*** conditions, for different species indicating differences species behavioral responses.

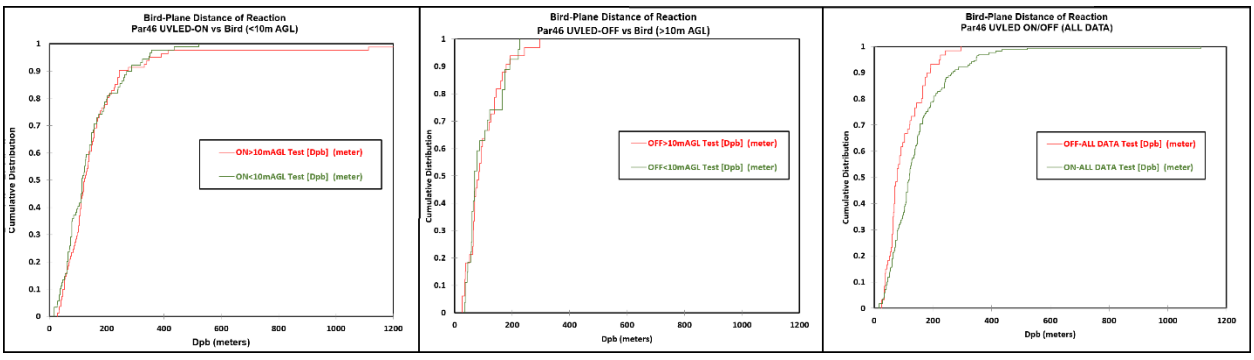

Figure 12. The cumulative distribution are similar for reaction distance to plane with ***PAR46$_{UVLED}$*** for the ***ON*** vs ***OFF***: greater than or less than 10meters ***AGL***

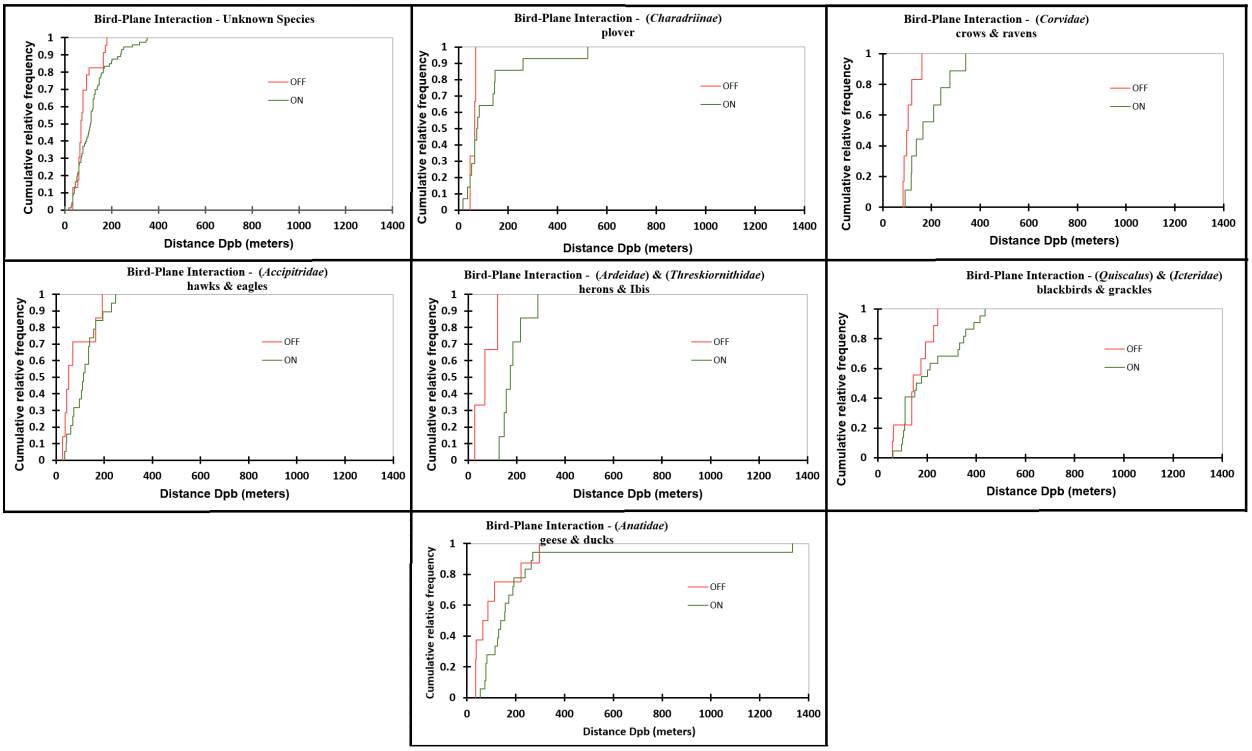

Figure 13. The cumulative distribution of species subsets for the birds' reaction distance to the plane with ***PAR46$_{UVLED}$*** either ***ON*** or ***OFF***

The descriptive statistics of different species in Table 4 identifies that the ***Dpb*** (distance at the moment of plane-bird reaction) varies greatly between species.

Table 4. Descriptive statistics of species distance of response (D_{pb}) (meters)

Species	**PAR46$_{UVLED}$ *ON* (mean, n)**	**PAR46$_{UVLED}$ *OFF* (mean, n)**
(*Anatidae*) geese & ducks	(214, 18)	(112, 8)
(*Passerine*) small body	(75,5)	(-,0)
(*Icteridae*) (*Quiscalus*) blackbirds & grackles	(212, 22)	(153, 9)
(*Ardeidae*) (*Threskiornithidae*) Herons & Ibis	(185,7)	(72, 3)
(*Accipitridae*) hawks & eagles	(119, 19)	(84, 7)
(*Corvidae*) crows & ravens	(189, 9)	(109, 6)
(*Charadriinae*) plover	(123, 14)	(60, 3)
unknown	(119, 73)	(85, 23)
(*Cathartidae*) vulture	(182, 1)	(-,0)

1.2.9 First field trial – predictive distance model – ***ON*** versus ***OFF***

A multivariable linear regression model used a linear regression framework to predict the distance of reaction (***PDpb***) as the dependent variable with only field recorded data as the independent variables resulted in a low significance of correlation ($R2 = 0.146$). Flock size, weather conditions, temperature, wind direction, wind speed, time, date, cloud cover, precipitation, and illuminance measurements weakly correlated as independent variables. The linear regression analysis of each of the three independent variables (***V***1, ***V***2, and ***V***3) are strongly correlated to ***Dpb*** (−0.5236, −0.8674, −0.7236, $n = 75$) (see Table 5). This led to the determination of three variables (***V***1, ***V***2, and ***V***3) to examine the sequential regions involved in the avian visual processing system.

Table 5. Correlation of modeled variables – all empiracally derived data

	Ee	***SNR***	***ON/OFF***	V_1	V_2	V_3	D_{pb}
Ee	1						
SNR	0.99858	1					
ON/OFF	0.11085	0.12824	1				
V_1	0.50046	0.49294	-0.41562	1			
V_2	0.30602	0.30108	-0.63134	0.84178	1		
V_3	0.40728	0.40005	-0.57364	0.94349	0.96762	1	
D_{pb}	-0.12806	-0.12981	0.55671	-0.52358	-0.86743	-0.72355	1

The three independent variables (***V***1, ***V***2, and ***V***3) used to derive the coefficients, and intercept values (***PDpb***) for the predicted rate of change of Equation 7 were significant probabilities (p-values for Intercept, ***V***1, ***V***2, and ***V***3 are 5.969 E−66, 2.043 E−19, 1.219 E−48, and 6.577 E−35, respectively) (see Table 6). The resulting equation to the predicted distance of plane-bird interaction (***PDpb***) value is described as:

$$\boldsymbol{PDpb = 1041 + (-7)(V1) + (-1541)(V2) + (683)(V3)} \quad 7$$

Table 6. Coefficients of modeled variables for distance of plane bird interaction (PD_{pb})

	Coefficients	**Standard Error**	***T* stat**	***P*-value**	**Lower 95%**	**Upper 95%**
Intercept	1041.32999	15.527593	67.06319	5.969E−66	1010.3688	1072.2911
***V*1**	−6.981792	0.5636363	−12.38705	2.043E−19	−8.105651	−5.857933
***V*2**	−1541.101	40.952002	−37.63188	1.219E−48	−1622.757	−1459.445
***V*3**	683.08214	29.397344	23.236185	6.577E−35	624.4655	741.69878

The linear regression of these three variables were strongly significant in predicting the distance of reaction to the approaching plane for either condition of the lights ***ON*** or ***OFF***. The ***V***2 and ***V***3 variables are the more dominant with greater significance of correlation of the three variables (***V***1, ***V***2, and ***V***3). ***PHeye*** (or ***V***1) is the postulated number of horizontal cell groups of the eye involved in the detection of the plane's wingspan at distance (***Dpb***) (i.e., analogous to image formation on a detector's surface). The ***FI*** brightness of the background sky from the perspective of the bird is the dominant variable in calculating ***SNR***. Note that the ***FI*** value applied to the ***I*** value significantly differentiates the 75 dataset ***SNR*** values, which is carried forward by the ***V***2 and ***V***3 values. ***V***2 is the logarithmic addition of ***PHeye*** with ***SNR*** involving retinal image signal processing (i.e., analogous to kernel or convolution matrix amplification). ***V***3 is the result of multiplying ***V***2 by ***V***2, involving complex signal processing of the brain, optical nerves, and retinal neurons (i.e., analogous to the Euclidean vector that has a geometric object with magnitude and direction values).

The combined ***ON***/***OFF*** dataset of the three independent variables (***V***1, ***V***2, and ***V***3) were significantly correlated to ***PDpb*** ($R2 = 0.9941$, $n = 75$). The interaction distance for each group of ***ON***/***OFF*** were significant, correlated to ***PDpb*** ($R2 = 0.9877, 0.9733$, $n = 43, 32$) (see Figure 14).

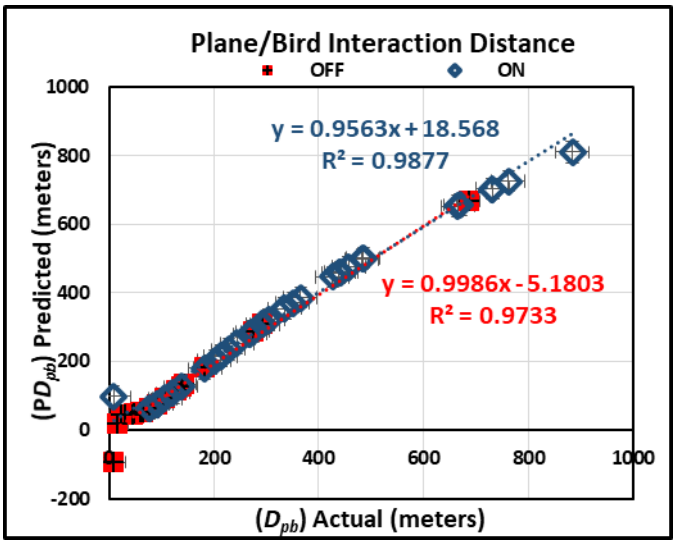

Figure 14. Predicted distance of bird reaction – ***PAR46$_{UVLED}$*** turned either **ON** or **OFF**

1.2.10 Second field trial – predictive distance model – *ON* versus *OFF*

A multivariable linear regression model analysis, described in section 1.2.9, using a linear regression framework to predict the distance of reaction (***PDpb***) as the dependent variable, resulted in the three independent variables (***V***1, ***V***2, and ***V***3) strongly correlated to ***Dpb*** (−0.528, −0.806, −0.691, $n = 228$) (see Table 7). Flock size, weather conditions, temperature, wind direction, wind speed, time, date, cloud cover, precipitation, and illuminance measurements weakly correlated as independent variables and not utilized in this predictive model.

Table 7. Correlation of all empirally derived variables (from all data)

	Ee	***SNR***	***ON/OFF***	V_1	V_2	V_3	D_{pb}
Ee	**1**						
SNR	0.637	**1**					
ON/OFF	0.223	0.258	**1**				
V_1	0.763	0.536	-0.136	**1**			
V_2	0.521	0.440	-0.199	0.889	**1**		
V_3	0.604	0.485	-0.186	0.952	0.982	**1**	
D_{pb}	-0.240	-0.236	0.171	-0.528	-0.806	-0.691	**1**

The three independent variables (***V***1, ***V***2, and ***V***3) used to derive the coefficients, and intercept values (***PDpb***) for the predicted rate of change of Equation 8 were significant probabilities (*p*-values for Intercept, ***V***1, ***V***2, *and* ***V3*** are all <0.0001, respectively) (see Table 8).

Table 8. Predicted distance of plane bird interaction (PDpb) – significant model parameters

	Coefficients	Standard Error	T Stat	P-value	Lower 90%	Upper 90%
Intercept	1628.349	16.904	96.329	<0.0001	1600.429	1656.269
V_1	-8.217	0.319	-25.726	<0.0001	-8.744	-7.689
V_2	-2269.781	32.866	-69.062	<0.0001	-2324.06486	-2215.49636
V_3	934.217	18.988	49.201	<0.0001	902.855	965.579

The resulting equation to the predicted distance of plane-bird interaction (***PDpb***) value is described as:

$$\boldsymbol{PDpb = 1628 + (-8.2)(V1) + (-2269.8)(V2) + (934.2)(V3)} \quad 8$$

The entire ***ON/OFF*** dataset of the three independent variables (***V***1, ***V***2, and ***V***3) were significantly correlated to ***PDpb*** (R^2 = 0.985, n = 228). The interaction distance for each group of ***ON/OFF*** were significant correlated to ***PDpb*** (R^2 = 0.9847, 0.9734, n = 170, 60) (see Figure 15).

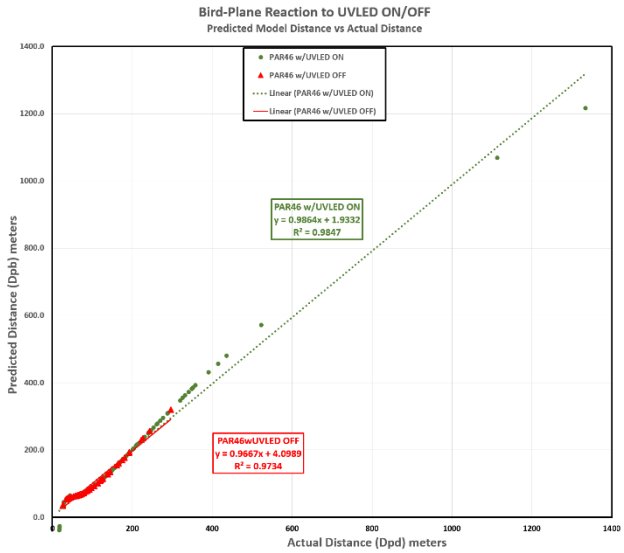

Figure 15. Predicted distance of bird reaction – ***PAR46$_{UVLED}$*** turned either ***ON*** or ***OFF***

Correlation of modeled variables for ***Dpb*** and ***PDpb*** for plane-bird distance were organized into species data subsets (see Table 9). All subsets species ***Dpb*** and ***PDpb*** data points were highly correlated within their species group: (R^2 = 0.9966, 0.9966, 0.9852, 0.9688, 0.9979, 0.9858, n = 26, 31, 10, 26, 15, and 17 for geese & ducks (*Anatidae*), blackbirds & grackles (*Icteridae*) + (*Quiscalus*), Herons & Ibis (*Ardeidae*) + (*Threskiornithidae*), hawks & eagles (*Accipitridae*),

crows & ravens (*Corvidae*), plover (*Charadriinae*) species groups, respectively). The small body (*Passerine*), vulture (*Cathartidae*), and unknown subsets had small sample numbers or unknown species and were not analyzed (see Figure 16).

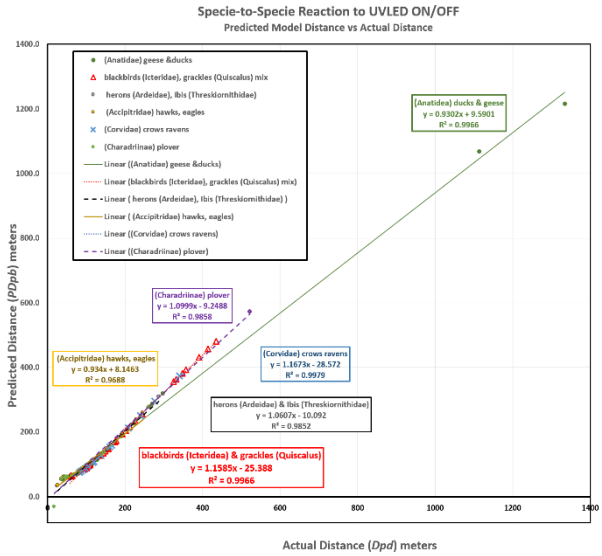

Figure 16. Predicted distance of bird reaction of ***PAR46$_{UVLED}$ ON*** or ***OFF*** for each species data subset

Table 9. Descriptive statistics by species distance of response (D_{pb}) (meters)

Species	***Linear equation***	**R^2 value**
(*Anatidae*) geese & ducks	y = 0.9302x + 9.5901	0.9966
(*Passerine*) small body	-	-
(*Icteridae*) + (*Quiscalus*) blackbirds & grackles	y = 1.1585x - 25.388	0.9966
(*Ardeidae*) + (*Threskiornithidae*) Herons & Ibis	y = 1.0607x - 10.092	0.9852
(*Accipitridae*) hawks & eagles	y = 0.934x + 8.1463	0.9688
(*Corvidae*) crows & ravens	y = 1.1673x - 28.572	0.9979
(*Charadriinae*) plover	y = 1.0999x - 9.2488	0.9858
unknown	-	-
(*Cathartidae*) vulture	-	-

2 Comments and recommendations

The operation concept enables the ***PAR46$_{UVLED}$*** landing lights to be operated at the pilot's discretion. The device does not require active control by the pilot to increase flight path separation thereby enabling a reduced risk of bird strikes. The pilot remains responsible to operate the landing lights in compliance with all regulations and operational procedures requirements.

- The pilots' situational awareness to a flight operation in an environment that presents opportunities for bird encounters should lead to the powering the ***PAR46$_{UVLED}$***.
- The pilots' situational awareness to an increased risk of a bird encounter should increase the pilots' attention to the airspace surrounding the rotorcraft and preparedness for avoidance maneuvers.

The model was designed by analyzing current literature on avian neurophysiology to develop an effective method of increasing flight path separation between birds and air vehicles. The data collected throughout this study was conducted during daylight. The empirically derived model predicts the effectiveness of the device to increase the ***PDpb*** during nighttime vs. daytime operations due to the increased ***SNR*** (signal-to-noise ratio) of the landing light. It is noted that the ***SNR*** value is poorly correlated to predicted distance by itself.

The author recommends further study to evaluate the effectiveness of the ***PAR46$_{UVLED}$*** to varying flight conditions and species, as follows:

- Nighttime conditions
- Varying climate and weather conditions
- Varying species flying at higher altitudes
- Wider range of bird species

2.1 System overview

This study demonstrated increased flight path separation between bird and air vehicles with ***PAR46$_{UVLED}$*** landing light turned ***ON*** vs ***OFF***. The goal of increased flight path separation is to reduce bird strikes resulting from the bird's increased awareness and quicker behavioral responses to the approaching air vehicle.

The device utilized in these field trials involved a prototype landing light with three colors of UVLEDs, which were independently pulsed while operating as a white light PAR46 landing light. The prototype landing light is designed to be readily installed and operated in any air vehicle without requiring special modifications or adding to the pilot's workload. The first set of

field trials involved a ¼-scale remote controlled ***RC*** plane while the second set of field trials involved an AirTractor 802 aircraft performing flight operations at nominal flight speeds of 150 kt and < 100' ***AGL*** in the performance of agricultural chemical delivery. The ultraviolet light emitting diodes (**UVLEDs**) do not impede the function of the landing light or interfere with the operation or safety of the air vehicle.

A statistically significant increase in ***Dpb*** was measured in both field trials when the $PAR46_{UVLED}$ was powered. The variables measuring the device and the environment (temp, clouds, species, flock structure, etc.) were studied. An empirically derived model consistent with modern neurophysiological research involved three empirically derived variables (***V*1, *V*2,** and ***V*3)** corresponding to three sequential steps; sensory perception, cognitive recognition, and reaction was highly correlated with ***PDpb***. The airspeed of the air vehicle and other environmental values were poorly correlated to ***PDpb***. The bird location (on the ground, altitudes <10m ***AGL***, or altitudes >10m ***AGL***) with the ***Dpb*** was poorly correlated. Flock size was poorly correlated to ***PDpb***.

The linear regression of these three variables were strongly significant in predicting the distance of reaction to the approaching plane for either condition of the lights ***ON*** or ***OFF***. The ***V***2 and ***V***3 variables are the more dominant variables, with a greater significance of correlation of the three variables (***V***1, ***V***2, and ***V***3). ***PHeye*** or ***V***1 is the postulated number of horizontal cell groups of the eye involved in the detection of the plane's wingspan at distance (***Dpb***) (i.e., analogous to image formation on a detector's surface). The ***FI*** brightness of the background sky from the perspective of the bird is the dominant variable in calculating ***SNR***. Note that the ***FI*** value applied to the ***I*** value significantly differentiates the dataset **SNR** values, which are carried forward by the ***V***2 and ***V***3 values. ***V***2 is the logarithmic addition of ***PHeye*** with ***SNR***, and corresponds to retinal image signal processing (i.e., analogous to kernel or convolution matrix amplification). ***V***3 is the result of multiplying ***V***2 by ***V***2, and corresponds to complex signal processing of the brain, optical nerves, and retinal neurons (i.e., analogous to the Euclidean vector that has a geometric object with magnitude and direction values). These field trials results and the model's validation of modern neuroscience studies add great insight to the neurophysiological process. While the optical, engineering principles, and lateral inhibition of neurons are widely acknowledged, the cognitive behavioral response is less well understood.

Species data subset analysis identified variation between mean distances recorded by ***Dpb*** and illustrated by the plot of cumulative distribution to the $PAR46_{UVLED}$, indicating significant species differences, which is well correlated to the PDpb of the three variable model for all

species measured. It is postulated the differences are related to physiological and behavioral differences of species.

The dominance of geese & ducks (*Anatidae*) measured in Field Test #1 is attributed to the comparative difference with the mean ***Dpb*** values of Field Test #2, which involved a diverse range and number of species.

An under sampling of some species, especially species with small body sizes, is postulated to be the result of the resolution limitations of the camera system. Plots of cumulative distribution of species data subsets supported with the mean value offsets for similar body sized birds (e.g. crows & ravens (*Corvidae*) vs. plover (*Charadriinae*), etc.) demonstrates species differences.

The diversion behavior observed consisted of changing flight direction or flight behavior to the approaching plane. Various anecdotal observations (i.e. raptors initial response often begins with what appears to be a head-on defensive response attack flightpath before altering to an evasive flight direction) further support the postulated theory that various species will exhibit differing behaviors and ***Dpb***. A limited number of head-on interactions with the ***PAR46$_{UVLED}$*** landing light ***ON*** were recorded where organized V-shaped geese flocks would split and fly in opposing directions, or even reverse their flight direction. The agricultural pilot observed that when encountering foraging duck species in the fields during chemical applications with the AirTractor 802 configured with standard blinking 'wing-wag' landing lights, they would usually move a short distance but would be slow in leaving the area. The foraging duck behavior was different when the AirTractor 802 configured with ***PAR46$_{UVLED}$*** was turned ***ON***. The foraging duck species would usually leave the area after the first fly. The reaction of very large well-organized flocks of geese tended to react as individuals when illuminated by the ***PAR46$_{UVLED}$*** but quickly regrouped the flock structure when they exited the field of illumination.

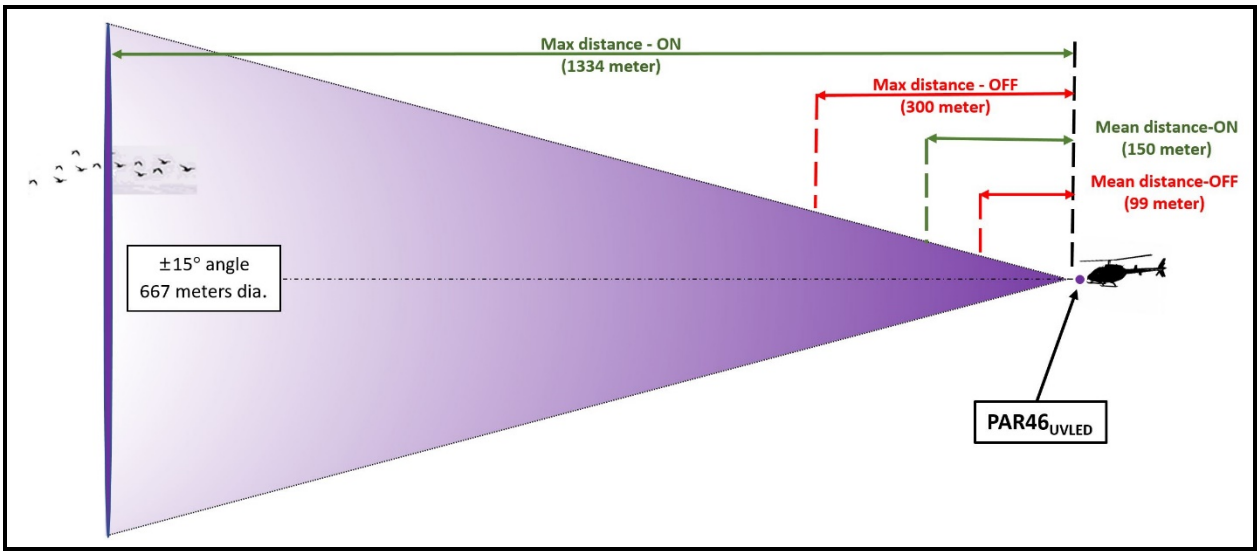

Figure 17. Illustration of airspace separation between the plane and the birds

This project is the first to study wild birds in a natural environment interacting midair with an aircraft and measure the difference in the bird's distance of response to an approaching plane, operating at a nominal speed of 150 kt with ***PAR46$_{UVLED}$*** landing lights ***ON*** versus ***OFF*** resulting in increased flight path separation (see Figure 17). A statistical correlation of predictable distance of response to a three-variable model representing a bird's eye visual capture ability of the plane, the retinal neural coding ability, and the complex nonlinear neural response of the brain to the visual input suggested by recent advances in knowledge of avian vision was established. When the birds were illuminated by the ***PAR46$_{UVLED}$ ON***, a stronger behavioral response was seen at a greater distance than when the lights were ***OFF***. For a plane traveling at 77 m/s, the mean reaction distance with the ***PAR46$_{UVLED}$ OFF*** is 199.8 m, compared to the ***PAR46$_{UVLED}$ ON*** mean reaction distance of 152.7 m. In this study the maximum distance in which the ***PAR46$_{UVLED}$ ON*** caused the birds to react was 1334 m compared to ***PAR46$_{UVLED}$ OFF*** distance of 296 m.

3 References

1. Fact Sheet – The Federal Aviation Administration's Wildlife Hazard Mitigation Program https://www.faa.gov/news/fact_sheets/news_story.cfm?newsId=14393.

2. Federal Aviation Administration National Wildlife Strike Database Serial Report Number 24, Wildlife Strikes to Civil Aircraft in the United States, 1990–2017, January 2019, page v-vii).

3. Stadtmueller, T., "Rotorcraft Bird Strike Data," Dec. 2016, DOT/FAA/TC-TN16/48. This document is available to the U.S. public through the National Technical Information Services (NTIS), Springfield, Virginia 22161. This document is also available from the Federal Aviation Administration William J. Hughes Technical Center at actlibrary.tc.faa.gov.

4. Soldatini, C. In: DeVault T., Blackwell B., and Belant J., editors. Wildlife in Airport Environments: Preventing Animal-Aircraft Collisions through Science-Based Management. (Baltimore, MD, Johns Hopkins University Press, 2013), doi:10.1111/jofo.12073_5.

5. McKee J., Shaw P., Dekker A., Patrick K. (2016) Approaches to Wildlife Management in Aviation. In: Angelici F. (eds) Problematic Wildlife. Springer, Cham, doi:10.1007/978-3-319-22246-2_22.

6. Witzel, C., and Gegenfurtner, K. (2015), "Chromatic Contrast Sensitivity in Luo, R. et al.," Encyclopedia of Color Science and Technology, doi:10.1007/978-3-642-27851-8_17-1.

7. Stoddard, M.C. and Prum, R.O. , "Evolution of Avian Plumage Color in a Tetrahedral Color Space: A Phylogenetic Analysis of New World Buntings," The American Naturalist 171(6):755-776, 2008, doi:10.1086/587526.

8. Morena, L., Diaz, N., Guido, M. "Chick retinal horizontal cell photoreceptor", Proceedings of the National Academy of Sciences, 2016, 113 (46) 13215-13220; doi: 10.1073/pnas.1608901113.

9. Hunt, D., Peichl, L., "S Cones: Evolution, Retinal Distribution, Development, and Spectral Sensitivity," Visual Neuroscience 31, no. 2 (2014): 115–38. doi:10.1017/S0952523813000242.

10. Mitkus, M. “Spatial Vision in Birds: Anatomical Investigation of Spatial Resolving Power,” *Lund University Publications*, 2015, https://lup.lub.lu.se/search/publication/7865188.

11. Wylie, D., Gutiérrez-Ibáñez, C., et al., Visual-Cerebellar Pathways and Their Roles in the Control of Avian Flight, Front. Neurosci., 09 April 2018, doi:10.3389/fnins.2018.00223.

12. Lischka, K., Simone L., et al, "Expression patterns of ion channels and structural proteins in a multimodal cell type of the avian optic tectum." *Journal of Comparative Neurology* 526, no. 3 (2018): 412-24, accessed March 2019, https://onlinelibrary-wiley-com.ezproxy.neu.edu/doi/pdf/10.1002/cne.24340.

13. Jarvis ED, Güntürkün O, Bruce L, et al. Avian brains and a new understanding of vertebrate brain evolution. *Nature Reviews Neuroscience*. 2005;6(2):151-9, doi: 10.1038/nrn1606.

14. McLeod, S. “Visual Perception Theory”, Simply Psychology, accessed March 2019, https://www.simplypsychology.org/perception-theories.html.

15. Shimizu T, Bowers AN, Visual circuits of the avian telencephalon: evolutionary implications, *Behavior Brain Research*, February 1999; 98 (2) 183-191, doi: 10.1016/S0166-4328(98)00083-7.

16. Wylie, D., Gutiérrez-Ibáñez, C. et al, “Visual-Cerebellar Pathways and Their Roles in the Control of Avian Flight,” Frontiers in Neuroscience 12:223, 2018, doi:10.3389/fnins.2018.00223.

17. Rubene, D., Hastad, O., Tauson, H., et al. “The presence of UV wavelengths improves the temporal resolution of the avian visual system,” Journal of Experimental Biology, 2010, 213: 3357-3363; doi: 10.1242/jeb.042424.

18. Odeen, A., Hastad, O., “The phylogenetic distribution of ultraviolet sensitivity in birds,” BMC Evolutionary Biology, no.13 (2013) 1- 10, doi: 10.1186/1471-2148-13-36.

19. Eugen, K., et al, “A comparative analysis of the dopaminergic innervation of the executive caudal nidopallium in pigeon, chicken, zebra finch, and carrion crow”, *J Comp Neurol*, 2020:S28.2929-2955 doi:10.1002/cne.24878.

20. Yi-Tse, H., et al, “Connectivity between nidopallium caudolateral and viual pathways in color perception of zebra finches”, *Scientific Reports* 2020, Nov 9;10(1):19382, doi: 10.1038/s41598-020-76542-z.

21. Knudson. E., Schwarz,J., Reference Module in Neuroscience and Biobehavioral Psychology, Evolution of Nervous Systems, 2nd ed, Vol 1., (Stanford: Stanford University School of Medicine, 2017), 387-408, doi: 10.1016/B978-0-12-804042-3.00016-6.

22. Dwyer, J, et al, " Near ultraviolet light reduced Sandhill Crane collisions with power line by 98%.", *The Condor*, Volume 121, Issue 2, 1 May 2019, duz008, https://doi.org/10.1093/condor/duz008.

23. Egan, C, et al, "Testing a key assumption of using drones as frightening devices: Do birds perceive drones as risky?", *The Condor*, 122, no. 3 (2020): 1-15.doi:10.1093/condor/duaa0.

A Field data and derived values

					Feb-Apr 2021 FAA Test @ Fisher, AR (Whirlwind Aviation)								Plane: AirTractor 810									k1=300 lux@ k2 distance			k2=30'=9.375m		k3.2=18.06m		tan(0.5°)=0.008726			
			end - vid	Dist = sec	Video time	Date	Event #	Temp (F)	Wind (mps)	[I] (lux)	Cloud Cover	Plane Direction	Plane speed (mps)	Species	Flock size	Plane (AGL)	Bird Direction	Bird speed (mps)	Bird (AGL)	$[F_i]$	Head-on Flight	Sun-Plane Backlit	$[Ee]$	SNR	ON/OFF PAR46	$[V_i]$ or $[PH_{eye}]$	$[V_2]$	$[V_3]$	Test $[Dpb]$ (meter)	Linear V1 V2 V3: Pred([Dpb] (meter)	PAR46 UVLED
4	1	1.5	16	1334	GH050130 9	2/25/2021	33	50	7.0	700	3	6	77	2	40	200	8	15.0	250	1.25	2	0	0.0	1.0000	1	1.6	0.1908	0.04	1334.0	1216.626	ON
5	2.1	3.3	4	64.4	GH080130 1	2/25/2021	35	50	7.0	700	3	6	77	3	50	200	2	15.0	230	1.25	2	0	6.0	1.0068	1	32.1	1.5100	2.28	64.4	67.014	ON
6	3.6	3.9	16	1113.2	GH030130 1	2/25/2021	31	50	7.0	1100	2	6	77	1	100	200	7	15.0	150	1.25	1	0	0.0	1.0000	1	1.9	0.2693	0.07	1113.2	1069.509	ON
7	0	4.1	6.2	182.7	GH020031 2	3/8/2021	77	64	9.0	1650	0	1	77	10	6	15	1	10.0	150	1.00	2	0	0.7	1.0005	1	11.3	1.0544	1.11	182.7	180.649	ON
8		7.9	8.6	60.9	GH010 19 -8	1/18/2021	2	62	9.0	1650	0	7	77	9	1	5	1	10.0	100	8.00	2	7	6.7	1.0005	1	34.0	1.5315	2.35	60.9	64.142	ON
9	0.1	2.1	4.6	230	GH020029 5	3/4/2021	58	65	5.0	1650	0	5	77	6	1	150	1	15.0	100	1.00	2	0	0.5	1.0003	1	9.0	0.9543	0.91	230.0	239.141	ON
10	0	1.8	3.6	156.6	GH010168 1	3/16/2021	122	72	7.0	1400	1	1	77	4	2	3	6	10.0	100	6.50	2	0	1.0	1.0001	1	13.2	1.1212	1.26	156.6	149.279	ON
11	7	9	19	60	GN110130 m	2/25/2021	36	50	7.0	700	3	5	0	4	1000	0	1	6.0	70	8.00	2	0	6.9	1.0012	1	34.5	1.5383	2.37	60.0	64.009	ON
12	0	0.4	0.9	43.5	GH030034 1	4/30/2021	207	65	4.0	1650	0	5	77	9	1	50	7	10.0	60	2.50	1	0	13.1	1.0032	1	47.6	1.6788	2.82	43.5	59.869	ON
13		13.4	15.2	153	GH010 19 -1	1/18/2021	4	62	9.0	1650	0	3	77	9	100	5	1	8.0	50	1.25	2	7	1.1	1.0005	1	13.5	1.1314	1.28	153.0	145.025	ON
14		10.2	11.4	102	GH010 19 -9	1/18/2021	3	62	9.0	1650	0	3	77	9	30	5	5	8.0	50	1.25	2	7	2.4	1.0012	1	20.3	1.3078	1.71	102.0	91.038	ON
15	1.8	2.2	3.4	110.4	GH040019 1	1/18/2021	23	50	7.0	1100	1	3	77	4	100	5	6	15.0	50	2.50	1	1	2.0	1.0007	1	18.7	1.2733	1.62	110.4	98.835	ON
16	0	1.4	3.2	165.6	GH020161 0	3/22/2021	131	72	7.0	1100	1	3	77	6	1	50	4	15.0	50	1.25	1	0	0.9	1.0007	1	12.5	1.0971	1.20	165.6	159.925	ON
17	0	0.4	2.5	193.2	GH020161 0	3/22/2021	130	72	7.0	1100	1	1	77	6	1	50	6	15.0	50	1.25	1	0	0.7	1.0005	1	10.7	1.0301	1.06	193.2	193.528	ON
18	0	11.5	16.6	331.5	GH010150 1	3/4/2021	51	44	7.0	1650	0	5	50	4	30	5	7	15.0	40	1.25	1	0	0.2	1.0001	1	6.2	0.7955	0.63	331.5	362.657	ON
19	0	4.8	6.1	119.6	GH060032 1	3/8/2021	81	64	9.0	1650	0	3	77	6	1	10	1	15.0	40	8.00	1	0	1.7	1.0001	1	17.3	1.2382	1.53	119.6	108.005	ON
20	0	3.9	5	88	GH080018 1	4/22/2021	186	52	3.0	1650	0	1	60	9	1	25	5	20.0	40	8.00	1	1	3.2	1.0002	1	23.5	1.3715	1.88	88.0	79.379	ON
21	0	1	3.6	239.2	GH210167 2	3/16/2021	127	72	7.0	1100	1	3	77	9	200	10	6	15.0	40	2.50	0	0	0.4	1.0001	1	8.7	0.9372	0.88	239.2	250.587	ON
22	0	1.7	3.2	138	GH030152 3	3/8/2021	66	42	3.0	1650	0	2	77	2	20	30	3	15.0	40	1.25	0	5	1.3	1.0006	1	15.0	1.1763	1.38	138.0	127.835	ON
23	0	1.4	2.7	119.6	GH012703 1	3/29/2021	149	72	7.0	1650	0	5	77	7	3	30	8	15.0	40	2.50	1	0	1.7	1.0004	1	17.3	1.2384	1.53	119.6	108.010	ON
24	1	1.2	2	73.6	GH050019 1	1/18/2021	24	50	7.0	1100	1	7	77	6	1	5	6	15.0	40	6.50	1	0	4.6	1.0006	1	28.1	1.4493	2.10	73.6	69.997	ON
25	0	1	1.8	77.6	GH080152 0	3/8/2021	69	42	3.0	1650	0	7	77	2	5	60	1	20.0	40	6.50	0	0	4.1	1.0004	1	26.7	1.4262	2.03	77.6	72.286	ON
26	0	1.2	4.8	216	GH030147 5	3/2/2021	45	44	7.0	700	3	5	60	5	1	35	7	0.0	35	1.00	1	0	0.5	1.0008	1	9.6	0.9818	0.96	216.0	221.678	ON
27	0	26.2	27.8	120	GH010150 2	3/4/2021	54	44	7.0	1650	0	5	60	9	1	10	7	15.0	30	6.50	0	0	1.7	1.0002	1	17.2	1.2368	1.53	120.0	108.418	ON
28	0	25	26.4	105	GH010150 2	3/4/2021	53	44	7.0	1650	0	5	60	9	1	10	7	15.0	30	6.50	2	0	2.3	1.0002	1	19.7	1.2948	1.68	105.0	93.700	ON
29	0	5.6	8.6	276	GH012705 7	4/6/2021	158	68	11.0	1650	1	5	77	7	1	5	7	15.0	30	2.50	1	0	0.3	1.0001	1	7.5	0.8750	0.77	276.0	295.918	ON
30	0	5.3	7.1	135	GH050012 7	4/12/2021	180	63	3.0	1650	0	1	60	6	1	20	3	15.0	30	2.50	1	0	1.4	1.0003	1	15.3	1.1857	1.41	135.0	124.503	ON
31	0	5	6.8	108	GH30167 15	3/16/2021	128	72	7.0	1100	1	5	50	9	1	15	1	10.0	30	6.50	2	0	2.1	1.0003	1	19.2	1.2826	1.65	108.0	96.515	ON
32	2.5	3.2	5.6	208.8	GH010164 4	3/16/2021	117	60	7.0	1400	1	5	77	7	5	30	1	10.0	30	1.25	1	0	0.6	1.0003	1	9.9	0.9963	0.99	208.8	212.833	ON
33	0	3.6	5.2	139.2	GH010156 5	3/8/2021	74	62	3.0	1650	0	3	77	6	1	5	8	10.0	30	1.25	0	0	1.3	1.0006	1	14.9	1.1725	1.37	139.2	129.182	ON
34	0	1.7	4.3	226.2	GH010168 8	3/16/2021	121	72	7.0	1400	1	1	77	9	2	5	2	10.0	30	6.50	0	0	0.5	1.0001	1	9.1	0.9614	0.92	226.2	234.471	ON
35	0	0.6	3.2	239.2	GH020160 1	3/22/2021	143	72	7.0	1100	1	5	77	7	1	10	7	15.0	30	2.50	1	0	0.4	1.0002	1	8.7	0.9372	0.88	239.2	250.575	ON
36	0	1.8	3.1	126.1	GH01270512	3/29/2021	147	72	7.0	1650	0	7	77	2	5	40	2	20.0	30	8.00	1	0	1.6	1.0001	1	16.4	1.2152	1.48	126.1	114.821	ON
37	0	0.7	2.5	149.4	GH20100 13	1/20/2021	18	50	7.0	1400	1	1	77	4	20	5	3	6.0	30	2.50	2	0	1.1	1.0003	1	13.9	1.1417	1.30	149.4	140.847	ON
38		0	1	83	GH020019 1	1/20/2021	20	50	7.0	1400	1	3	77	8	20	5	6	6.0	30	1.00	2	5	3.6	1.0026	1	24.9	1.3979	1.95	83.0	76.125	ON
39	0	2.6	6.6	348	GH010156 3	3/8/2021	73	62	3.0	1650	0	3	77	4	60	5	8	10.0	25	6.50	0	0	0.2	1.0000	1	5.9	0.7743	0.60	348.0	382.066	ON
40	0	4.4	6.3	165.3	GH010164 9	3/16/2021	118	60	7.0	1400	1	1	77	7	1	10	4	10.0	25	1.00	1	0	0.9	1.0006	1	12.5	1.0979	1.21	165.3	159.567	ON
41	0	2.1	5.8	340.4	GH020031 4	3/8/2021	78	64	9.0	1650	0	7	77	7	3	50	5	15.0	25	2.50	1	0	0.2	1.0001	1	6.1	0.7839	0.61	340.4	373.157	ON
42	0	3.6	5.3	68	GH030147 5	3/2/2021	43	44	7.0	700	3	5	20	9	1	0	7	20.0	25	2.50	1	7	5.4	1.0031	1	30.4	1.4847	2.20	68.0	67.661	ON
43	0	2.4	4.8	168	GH030147 2	3/2/2021	44	44	7.0	700	3	5	50	9	1	5	7	20.0	25	6.50	1	5	0.9	1.0002	1	12.3	1.0907	1.19	168.0	162.849	ON
44	0	3.2	3.9	53.9	GH080152 0	3/8/2021	72	42	3.0	1650	0	7	77	9	120	5	1	0.0	25	8.00	1	0	8.6	1.0006	1	38.4	1.5846	2.51	53.9	61.926	ON
45	0	2.1	3.5	135.8	GH022706 9	3/29/2021	147	72	7.0	1650	0	7	77	6	1	20	3	20.0	25	8.00	2	0	1.3	1.0001	1	15.2	1.1830	1.40	135.8	125.396	ON
46	0	0.1	2.3	202.4	GH010152 1	3/8/2021	63	42	3.0	1650	0	1	77	4	30	25	7	15.0	25	6.50	1	0	0.6	1.0001	1	10.2	1.0097	1.02	202.4	204.954	ON
47	5.2	5.2	12.3	390.5	GH020147 1	3/2/2021	42	44	7.0	700	3	1	40	4	40	3	3	15.0	20	2.50	1	0	0.2	1.0001	1	5.3	0.7243	0.52	390.5	430.878	ON
48	0	9.6	11.5	85.5	GH010150 1	3/4/2021	50	44	7.0	1650	0	5	45	1	1	0	3	0.0	20	1.25	0	0	3.4	1.0016	1	24.2	1.3847	1.92	85.5	77.734	ON
49	0	5.3	7.2	100.7	GH010167 1	3/16/2021	119	72	7.0	1400	1	5	50	4	2	0	3	3.0	20	8.00	1	0	2.4	1.0004	1	20.6	1.3131	1.72	100.7	89.825	ON
50	4.4	5.1	6.7	147.2	GH010147 6	3/2/2021	37	44	7.0	700	3	5	77	9	3	3	1	15.0	20	2.50	2	0	1.1	1.0007	1	14.1	1.1483	1.32	147.2	138.287	ON
51	0	0.8	6.7	177	GH010150 1	3/4/2021	49	44	7.0	1650	0	5	30	4	1	0	7	0.0	20	1.25	1	0	0.8	1.0004	1	11.7	1.0681	1.14	177.0	173.710	ON
52	0	3.5	6.6	108.5	GH020179 9	3/22/2021	139	72	7.0	1100	1	5	30	4	20	0	8	5.0	20	2.50	1	0	2.1	1.0005	1	19.1	1.2807	1.64	108.5	97.002	ON
53	0	1.2	5.7	414	GH040012 6	4/12/2021	178	63	3.0	1650	0	1	77	4	200	5	3	15.0	20	2.50	1	0	0.1	1.0000	1	5.0	0.6989	0.49	414.0	457.235	ON
54	0	2	4.8	243.6	GH012703 9	3/29/2021	147	72	7.0	1650	0	5	77	4	20	10	3	10.0	20	2.50	2	0	0.4	1.0001	1	8.5	0.9293	0.86	243.6	256.037	ON
55	1.2	2.8	4.3	138	GH010156 5	3/8/2021	75	62	3.0	1650	0	3	77	7	25	30	3	15.0	20	1.25	2	0	1.3	1.0006	1	15.0	1.1763	1.38	138.0	127.835	ON
56	0	3.1	4.3	110.4	GH040012 1	4/12/2021	179	63	3.0	1650	0	1	77	4	400	5	2	15.0	20	2.50	1	0	2.0	1.0005	1	18.7	1.2731	1.62	110.4	98.823	ON
57	0	3.5	4.1	52.2	GH020163 1	3/16/2021	126	72	7.0	1100	1	7	77	9	1	7	1	10.0	20	6.50	1	0	9.1	1.0009	1	39.6	1.5986	2.56	52.2	61.511	ON
58	0	1.6	4	96	GH070152 1	3/8/2021	68	42	3.0	1650	0	5	40	4	1	0	7	0.0	20	1.25	2	0	2.7	1.0013	1	21.6	1.3342	1.78	96.0	85.855	ON
59	0	0.9	2.7	156.6	GH020163 2	3/16/2021	124	72	7.0	1100	1	3	77	6	1	20	5	10.0	20	1.00	1	0	1.0	1.0009	1	13.2	1.1215	1.26	156.6	149.218	ON
60		0.4	1.6	104.4	GH020019 1	1/20/2021	19	50	7.0	1400	1	3	77	4	20	5	8	10.0	20	1.00	2	5	2.3	1.0016	1	19.8	1.2979	1.68	104.4	93.242	ON
61	0	0.3	1.6	97.5	GH020150 1	3/4/2021	61	52	3.0	1650	0	5	60	6	1	0	7	15.0	20	1.25	0	0	2.6	1.0013	1	21.2	1.3274	1.76	97.5	87.117	ON
62	22.8	23.5	24	46	GH01019 -13	1/18/2021	7	50	7.0	1650	0	7	77	9	30	5	3	15.0	15	8.00	2	7	11.7	1.0009	1	45.0	1.6535	2.73	46.0	59.811	ON
63	0	5.9	7.1	110.4	GH010007 5	4/8/2021	161	60	10.0	1650	0	5	77	4	40	5	8	15.0	15	2.50	2	0	2.0	1.0005	1	18.7	1.2731	1.62	110.4	98.823	ON
64	0	2.5	5.3	243.6	GH010163 1	3/16/2021	115	60	7.0	700	3	7	77	9	20	10	2	10.0	15	1.00	1	0	0.4	1.0006	1	8.5	0.9295	0.86	243.6	255.922	ON
65	3.7	3.7	4.7	92	GH020147 6	3/2/2021	38	44	7.0	700	3	5	77	7	60	40	7	15.0	15	1.00	0	0	2.9	1.0042	1	22.5	1.3539	1.83	92.0	82.919	ON
66	2.4	2.8	4.3	130.5	GH01019 -14	1/18/2021	9	50	7.0	1650	0	3	77	9	2	5	3	10.0	15	1.25	2	7	1.5	1.0007	1	15.9	1.2006	1.44	130.5	119.557	ON
67	3.6	3.7	4.3	55.2	GH01019 -14	1/18/2021	10	50	7.0	1650	0	7	77	9	2	5	3	15.0	15	8.00	2	7	8.2	1.0006	1	37.5	1.5742	2.48	55.2	62.296	ON
68	0	2.5	4.2	156.4	GH030161 0	3/22/2021	132	72	7.0	1100	1	3	77	2	30	10	4	15.0	15	1.25	1	0	1.0	1.0005	1	13.2	1.1219	1.26	156.4	149.015	ON
69	1	1.9	2.4	46	GH01019 -14	1/18/2021	8	50	7.0	1650	0	7	77	9	1	5	4	15.0	15	8.00	2	7	11.7	1.0009	1	45.0	1.6535	2.73	46.0	59.811	ON
70	0	0.2	2.4	202.4	GH010007 5	4/8/2021	160	60	10.0	1650	0	5	77	9	1	5	2	15.0	15	2.50	2	0	0.6	1.0001	1	10.2	1.0098	1.02	202.4	204.939	ON

72	0	0	1.35	117.45	GH012703 9	3/29/2021	146	72	7.0	1650	0	5	77	7	1	10	7	10.0	15	2.50	0	0	1.8	1.0004	1	17.6	1.2462	1.55	117.5	105.812	ON
73	0	0.3	3.2	174	GH012703 6	3/29/2021	145	72	7.0	1650	0	5	50	5	1	10	8	10.0	10	2.50	1	0	0.8	1.0002	1	11.9	1.0754	1.16	174.0	170.091	ON
74	0	1.6	3	121.8	GH010008 5	4/8/2021	165	60	10.0	1650	0	1	77	9	2	5	4	10.0	10	2.50	0	0	1.7	1.0004	1	17.0	1.2304	1.51	121.8	110.288	ON
75	0	2.4	3	52.2	GH010008 5	4/8/2021	166	60	10.0	1650	0	1	77	9	1	5	6	10.0	10	2.50	2	0	9.1	1.0022	1	39.6	1.5992	2.56	52.2	61.934	ON
76	0	1.1	2.8	147.9	GH010008 4	4/8/2021	164	60	10.0	1650	0	1	77	9	3	5	4	10.0	10	2.50	1	0	1.1	1.0003	1	14.0	1.1461	1.31	147.9	139.115	ON
77	0	1.2	2.4	104.4	GH020036 0	5/11/2021	212	53	4.0	1100	2	1	77	6	1	5	4	10.0	10	6.50	1	0	2.3	1.0003	1	19.8	1.2973	1.68	104.4	93.154	ON
78	1.2	1.4	1.9	41.5	GH02010 -2-	1/18/2021	12	50	7.0	1650	0	3	77	9	1	5	5	6.0	10	1.25	1	7	14.4	1.0070	1	49.9	1.7009	2.89	41.5	60.633	ON
79	0	0.8	1.6	69.6	GH030031 1	4/30/2021	206	65	4.0	1650	0	6	77	6	1	50	7	10.0	10	2.50	1	0	5.1	1.0012	1	29.7	1.4738	2.17	69.6	68.028	ON
80	0	0	1.4	128.8	GH032716 3	5/6/2021	210	66	3.0	1100	0	5	77	9	2	5	8	15.0	10	1.00	1	0	1.5	1.0014	1	16.1	1.2066	1.46	128.8	117.711	ON
81	0	0	1.3	113.1	GH010007 6	4/8/2021	163	60	10.0	1650	0	5	77	6	2	5	8	10.0	10	2.50	2	0	1.9	1.0005	1	18.3	1.2626	1.59	113.1	101.458	ON
82	0	0.8	1.2	34.8	GH012712 0	4/28/2021	198	74	9.0	1100	2	5	77	6	1	5	4	10.0	10	8.00	0	0	20.5	1.0023	1	59.5	1.7753	3.15	34.8	54.537	ON
83		0.1	0.6	41.5	GH020019 2	1/18/2021	22	50	7.0	1400	1	3	77	9	2	5	5	6.0	10	2.50	2	5	14.4	1.0041	1	49.9	1.6996	2.89	41.5	59.508	ON
84	0	0.1	0.5	28	GH080035 8	5/5/2021	208	68	4.0	1650	0	1	60	9	1	5	4	10.0	10	8.00	1	0	31.7	1.0024	1	73.9	1.8698	3.50	28.0	43.115	ON
85	0	1.3	5.3	348	GH050037 1	5/14/2021	217	50	5.0	1650	0	5	77	9	2	30	7	10.0	5	1.25	1	0	0.2	1.0001	1	5.9	0.7744	0.60	348.0	382.037	ON
86	0	4.1	4.6	41	GH020150 1	3/4/2021	59	52	3.0	1650	0	7	77	6	1	3	3	5.0	5	1.00	2	0	14.8	1.0090	1	50.5	1.7070	2.91	41.0	61.220	ON
87	0	2.4	4.6	191.4	GH050037 1	5/14/2021	216	50	5.0	1650	0	1	77	9	1	30	3	10.0	5	2.50	1	0	0.7	1.0002	1	10.8	1.0340	1.07	191.4	191.360	ON
88	0	3.6	4.1	43.5	GH020163 1	3/16/2021	125	72	7.0	1100	1	7	77	6	1	5	1	10.0	5	1.00	1	0	13.1	1.0188	1	47.6	1.6855	2.84	43.5	65.710	ON
89	0	1.2	3.5	200.1	GH050147 1	3/2/2021	47	44	7.0	700	3	3	77	9	30	5	5	10.0	5	6.50	0	0	0.6	1.0001	1	10.3	1.0147	1.03	200.1	202.096	ON
90	0	1.5	2.2	60.9	GH010007 5	4/8/2021	159	63	12.0	1100	0	5	77	6	1	5	2	10.0	5	2.50	0	0	6.7	1.0024	1	34.0	1.5323	2.35	60.9	64.638	ON
91	0	0.4	2.2	165.6	GH040010 1	4/9/2021	171	68	12.0	1650	0	1	77	9	1	5	3	15.0	5	2.50	1	0	0.9	1.0002	1	12.5	1.0969	1.20	165.6	159.967	ON
92	0	1	1.9	78.3	GH020037 1	5/14/2021	215	50	5.0	1400	0	1	77	9	15	15	5	10.0	5	2.50	1	0	4.1	1.0012	1	26.4	1.4226	2.02	78.3	72.849	ON
93	0	5.1	6.8	127.5	GH020150 9	3/4/2021	60	52	3.0	1650	0	1	65	5	1	0	3	10.0	3	6.50	2	0	1.5	1.0001	1	16.2	1.2105	1.47	127.5	116.320	ON
94	2.8	2.8	3.6	73.6	GH020147 8	3/2/2021	39	44	7.0	700	3	5	77	9	2	10	7	15.0	3	1.00	2	0	4.6	1.0066	1	28.1	1.4519	2.11	73.6	71.124	ON
95	1.1	2.2	3.5	113.1	GH020180 0	3/22/2021	141	72	7.0	1100	1	3	77	9	15	5	1	10.0	3	1.25	2	0	1.9	1.0014	1	18.3	1.2631	1.60	113.1	101.495	ON
96	0	21.2	23.2	140	GH010150 1	3/4/2021	52	44	7.0	1650	0	5	55	9	1	10	7	15.0	1	1.25	2	0	1.3	1.0006	1	14.8	1.1700	1.37	140.0	130.083	ON
97	0	0.4	2.2	156.6	GH010167 1	3/16/2021	120	72	7.0	1400	1	5	77	9	2	5	7	10.0	1	2.50	1	0	1.0	1.0002	1	13.2	1.1212	1.26	156.6	149.269	ON
98		21	22.1	84.7	GH010 19 -1	1/18/2021	6	50	7.0	1650	0	3	77	9	30	5	5	0.0	0	1.25	2	7	3.5	1.0017	1	24.4	1.3887	1.93	84.7	77.171	ON
99		20.4	20.6	17	GH010 19 -1	1/18/2021	5	62	9.0	1650	0	7	77	9	1	5	5	8.0	0	8.00	2	7	86.0	1.0065	1	121.7	2.0883	4.36	17.0	-37.895	ON
100	0	14	19.8	319	GH040007 7	4/8/2021	170	60	10.0	1100	0	1	40	9	30	5	6	15.0	0	2.50	1	0	0.2	1.0001	1	6.5	0.8122	0.66	319.0	347.835	ON
101	0	10.2	15.6	351	GH040007 7	4/8/2021	169	60	10.0	1650	0	1	50	9	30	5	6	15.0	0	2.50	2	0	0.2	1.0000	1	5.9	0.7706	0.59	351.0	385.554	ON
102	0	9.9	13.6	240.5	GH040007 7	4/8/2021	168	60	10.0	1650	0	1	50	9	30	10	6	15.0	0	2.50	1	0	0.4	1.0001	1	8.6	0.9348	0.87	240.5	252.198	ON
103	0	11.6	12.3	64.4	GH050001 0	3/30/2021	151	59	9.0	1650	1	7	77	3	10	5	7	15.0	0	8.00	0	0	6.0	1.0005	1	32.1	1.5072	2.27	64.4	65.495	ON
104		5.3	11.3	522	GH060130 1	2/25/2021	34	50	7.0	700	3	1	77	8	80	20	7	10.0	0	1.25	1	0	0.1	1.0001	1	4.0	0.5983	0.36	522.0	572.202	ON
105	0	7.8	9	110.4	GH03001 5-0	3/30/2021	149	59	9.0	1650	1	1	77	6	1	5	7	15.0	0	2.50	0	0	2.0	1.0005	1	18.7	1.2731	1.62	110.4	98.823	ON
106	0	1.7	8.1	288	GH010014 7	4/19/2012	181	58	7.0	1650	0	5	30	9	3	0	1	15.0	0	2.50	1	0	0.3	1.0001	1	7.2	0.8565	0.73	288.0	310.541	ON
107	2.8	5.2	7.8	239.2	GH020147 1	3/2/2021	41	44	7.0	700	3	2	77	2	150	150	4	15.0	0	2.50	2	0	0.4	1.0002	1	8.7	0.9372	0.88	239.2	250.555	ON
108		3.2	7.5	356.9	GH02099 -5-	1/18/2021	14	50	7.0	1100	2	3	77	4	100	5	5	6.0	0	6.50	2	5	0.2	1.0000	1	5.8	0.7634	0.58	356.9	392.420	ON
109	0	3.8	7.3	269.5	GH030161 1	3/22/2021	133	72	7.0	1100	1	3	77	2		60	5	0.0	0	1.00	0	0	0.3	1.0003	1	7.7	0.8855	0.78	269.5	287.900	ON
110		4.2	6.7	140	GH04099 -2-	1/18/2021	16	50	7.0	1100	2	1	50	8	20	15	3	6.0	0	2.50	2	0	1.3	1.0005	1	14.8	1.1700	1.37	140.0	130.088	ON
111	0	5.4	6.1	60.9	GH010163 1	3/16/2021	116	60	7.0	700	3	7	77	9	1	10	2	10.0	0	1.25	1	0	6.7	1.0077	1	34.0	1.5346	2.35	60.9	65.981	ON
112	0.9	1	6	435	GH20100 3-5	1/20/2021	17	50	7.0	1400	1	1	77	4	20	5	3	10.0	0	2.50	2	0	0.1	1.0000	1	4.8	0.6774	0.46	435.0	480.361	ON
113	0	3.9	5.6	139.4	GH020179 2	3/22/2021	138	72	7.0	1100	1	7	77	9	1	10	2	5.0	0	8.00	1	0	1.3	1.0001	1	14.8	1.1717	1.37	139.4	129.423	ON
114		1.58	5.5	325.36	GH02099 -5-	1/18/2021	13	50	7.0	1100	2	3	77	4	100	5	5	6.0	0	8.00	2	5	0.2	1.0000	1	6.4	0.8035	0.65	325.4	355.416	ON
115	0	4.1	5.3	110.4	GH010155 2	3/8/2021	76	62	3.0	1650	0	7	77	4	50	60	1	15.0	0	1.25	2	0	2.0	1.0010	1	18.7	1.2734	1.62	110.4	98.846	ON
116	0	4	5.1	71.5	GH030032 7	3/8/2021	80	64	9.0	1650	0	1	50	9	30	25	3	15.0	0	8.00	2	0	4.9	1.0009	1	28.9	1.4620	2.14	71.5	68.912	ON
117	4	4.4	4.8	36.8	GH020147 9	3/2/2021	40	44	7.0	700	3	5	77	9	2	10	7	15.0	0	6.50	2	0	18.3	1.0040	1	56.2	1.7518	3.07	36.8	56.967	ON
118	0	1.3	4.8	262.5	GH030152 1	3/8/2021	67	42	3.0	1650	0	1	60	2	20	30	3	15.0	0	6.50	0	0	0.4	1.0000	1	7.9	0.8968	0.80	262.5	279.378	ON
119	0	0.8	4.8	260	GH010036 1	3/8/2021	85	66	9.0	1650	0	5	50	8	40	25	3	15.0	0	6.50	1	7	0.4	1.0000	1	8.0	0.9009	0.81	260.0	276.301	ON
120	0	1.5	4.8	287.1	GH012704 1	3/29/2021	144	72	7.0	1650	0	1	77	5	1	5	3	10.0	0	2.50	0	0	0.3	1.0001	1	7.2	0.8579	0.74	287.1	309.447	ON
121	0	2.1	4.6	192.5	GH010179 1	3/22/2021	135	72	7.0	1100	1	7	77	2	12	20	5	0.0	0	6.50	2	0	0.7	1.0001	1	10.8	1.0315	1.06	192.5	192.724	ON
122	0	2.2	4.3	172.2	GH100168 1	3/16/2021	129	72	7.0	1100	1	3	77	2	20	30	3	5.0	0	1.25	2	0	0.8	1.0006	1	12.0	1.0801	1.17	172.2	167.867	ON
123	0	2.9	4.1	78	GH030034 1	3/8/2021	84	66	9.0	1650	0	1	50	8	40	25	3	15.0	0	6.50	1	0	4.1	1.0006	1	26.5	1.4241	2.03	78.0	72.564	ON
124	0	0.8	3.8	246	GH010179 7	3/22/2021	134	72	7.0	1100	1	7	77	6	1	5	2	5.0	0	6.50	2	0	0.4	1.0001	1	8.4	0.9250	0.86	246.0	259.017	ON
125	0	2.8	3.8	92	GH020012 8	4/19/2012	182	58	7.0	1650	0	6	77	9	1	30	3	15.0	0	8.00	1	0	2.9	1.0002	1	22.5	1.3522	1.83	92.0	82.474	ON
126	0	2.3	3.7	128.8	GH030152 3	3/8/2021	65	42	3.0	1650	0	1	77	2	6	30	3	15.0	0	6.50	2	0	1.5	1.0001	1	16.1	1.2060	1.45	128.8	117.720	ON
127	0	1.4	3.7	211.6	GH020034 1	3/8/2021	83	66	9.0	1650	0	1	77	4	60	20	3	15.0	0	6.50		0	0.6	1.0001	1	9.8	0.9904	0.98	211.6	216.353	ON
128	0	1.1	3.7	156	GH030018 5	4/22/2012	184	52	3.0	1650	0	1	50	5	1	15	5	10.0	0	8.00	2	1	1.0	1.0001	1	13.3	1.1228	1.26	156.0	148.575	ON
129	0	0.7	3.6	252.3	GH010029 2	3/4/2021	48	65	3.0	1650	0	7	77	9	2	30	1	10.0	0	8.00	2	0	0.4	1.0000	1	8.2	0.9140	0.84	252.3	266.809	ON
130	0	1.6	3.6	154	GH020179 1	3/22/2021	136	72	7.0	1100	1	5	77	2	12	20	5	0.0	0	6.50	1	0	1.0	1.0001	1	13.4	1.1284	1.27	154.0	146.221	ON
131	2.6	2.8	3.5	60.9	GH01019 -7-	1/18/2021	1	61	9.0	1650	0	7	77	9	6	5	5	10.0	0	8.00	2	0	6.7	1.0005	1	34.0	1.5315	2.35	60.9	64.142	ON
132	0	2.3	3.5	104.4	GH012711 1	4/28/2021	196	74	9.0	700	2	5	77	9	2	5	1	10.0	0	8.00	0	0	2.3	1.0004	1	19.8	1.2974	1.68	104.4	93.160	ON
133	0	1.2	3.4	202.4	GH020031 8	3/8/2021	79	64	9.0	1650	0	3	77	3	1	20	1	15.0	0	6.50	1	0	0.6	1.0001	1	10.2	1.0097	1.02	202.4	204.952	ON
134		0.7	3.3	145.6	GH04099 -2-	1/18/2021	15	50	7.0	1100	2	1	50	8	20	15	3	6.0	0	2.50	2	0	1.2	1.0004	1	14.2	1.1529	1.33	145.6	136.460	ON
135	0	2.5	3.3	61.6	GH080152 0	3/8/2021	71	42	3.0	1650	0	7	77	9	6	5	1	0.0	0	6.50	2	0	6.5	1.0006	1	33.6	1.5266	2.33	61.6	64.428	ON
136	0	0.9	3.1	121	GH060036 1	5/11/2021	214	53	4.0	1100	2	1	50	9	1	5	4	5.0	0	1.25	1	0	1.7	1.0012	1	17.1	1.2337	1.52	121.0	109.469	ON
137	0	0.5	2.9	184.8	GH010130 1	2/25/2021	30	50	7.0	1650	0	3	77	5	4	10	1	0.0	0	6.50	2	0	0.7	1.0001	1	11.2	1.0492	1.10	184.8	183.269	ON
138	0	2.2	2.9	64.4	GH020012 1	4/12/2021	175	63	3.0	1650	0	7	77	8	1	5	3	15.0	0	2.50	1	0	6.0	1.0015	1	32.1	1.5076	2.27	64.4	65.732	ON
139	0	1.2	2.8	124.8	GH010150 1	3/4/2021	56	44	7.0	1650	0	7	77	9	2	5	1	1.0	0	6.50	1	0	1.6	1.0001	1	16.6	1.2198	1.49	124.8	113.439	ON
140	0	1.5	2.8	113.1	GH012703 1	3/29/2021	152	72	7.0	1650	0	5	77	9	1	5	3	10.0	0	2.50	0	0	1.9	1.0005	1	18.3	1.2626	1.59	113.1	101.458	ON
141	0	1.4	2.8	121.8	GH012703 1	3/29/2021	143	72	7.0	1650	0	3	77	9	1	5	7	10.0	0	2.50	2	0	1.7	1.0004	1	17.0	1.2304	1.51	121.8	110.288	ON
142	0	1.2	2.8	147.2	GH030012 1	4/12/2021	176	63	3.0	1650	0	7	77	8	1	2	2	15.0	0	2.50	1	0	1.1	1.0003	1	14.1	1.1481	1.32	147.2	138.307	ON
143	0	0.9	2.7	147.6	GH010152 1	3/8/2021	62	42	3.0	1650	0	1	77	5	1	20	3	5.0	0	6.50	1	0	1.1	1.0001	1	14.0	1.1469	1.32	147.6	138.778	ON
144	0	0.4	2.7	188.6	GH010159 1	3/16/2021	123	72	7.0	1400	1	3	77	2	15	30	3	5.0	0	1.00	2	0	0.7	1.0005	1	11.0	1.0406	1.09	188.6	187.870	ON

145	0	2	2.7	64.4	GH020012 1	4/19/2012	183	58	7.0	1650	0	1	77	8	1	5	4	15.0	0	8.00	1	0	6.0	1.0005	1	32.1	1.5072	2.27	64.4	65.495	ON
146	0	1.3	2.7	121.8	GH062716 1	5/6/2021	211	66	3.0	1400	0	5	77	9	1	5	7	10.0	0	1.25	1	0	1.7	1.0010	1	17.0	1.2307	1.51	121.8	110.295	ON
147	0	1.6	2.5	78.3	GH040147 4	3/2/2021	46	44	7.0	700	3	3	77	2	5	5	1	10.0	0	6.50	1	0	4.1	1.0009	1	26.4	1.4225	2.02	78.3	72.804	ON
148	0	1.3	2.5	110.4	GH040012 5	4/12/2021	177	63	3.0	1650	0	1	77	9	1	5	4	15.0	0	2.50	1	0	2.0	1.0005	1	18.7	1.2731	1.62	110.4	98.823	ON
149	0	0.7	2.4	147.9	GH012711 1	4/28/2021	197	74	9.0	700	2	5	77	9	6	5	1	10.0	0	8.00	0	0	1.1	1.0002	1	14.0	1.1460	1.31	147.9	139.119	ON
150		0.8	2.3	124.5	GH020019 4	1/20/2021	21	50	7.0	1400	1	3	77	9	20	20	6	6.0	0	6.50	2	5	1.6	1.0002	1	16.6	1.2208	1.49	124.5	113.122	ON
151	0	1	2.3	100.1	GH080152 0	3/8/2021	70	42	3.0	1650	0	7	77	9	3	5	1	0.0	0	1.25	2	0	2.5	1.0012	1	20.7	1.3160	1.73	100.1	89.358	ON
152	0	0	2.2	165	GH040007 7	4/8/2021	167	60	10.0	1650	0	1	60	9	2	30	6	15.0	0	2.50	2	0	0.9	1.0002	1	12.5	1.0985	1.21	165.0	159.249	ON
153	0	1.6	2.1	46	GH020012 1	4/12/2021	174	63	3.0	1650	0	3	77	8	1	5	7	15.0	0	1.00	1	0	11.7	1.0071	1	45.0	1.6562	2.74	46.0	62.025	ON
154	0	0.5	2	115.5	GH020179 2	3/22/2021	137	72	7.0	1100	1	7	77	2	12	20	5	0.0	0	8.00	1	0	1.9	1.0001	1	17.9	1.2534	1.57	115.5	103.835	ON
155	0	0.7	2	113.1	GH022704 0	3/29/2021	145	72	7.0	1650	0	1	77	9	20	5	4	10.0	0	2.50	0	0	1.9	1.0005	1	18.3	1.2626	1.59	113.1	101.458	ON
156	0	0.6	1.9	113.1	GH020036 1	5/11/2021	213	53	4.0	1100	2	1	77	9	1	5	4	10.0	0	1.25	1	0	1.9	1.0014	1	18.3	1.2631	1.60	113.1	101.495	ON
157	0	0.9	1.8	73.8	GH020179 1	3/22/2021	140	72	7.0	1100	1	7	77	2	12	20	5	5.0	0	6.50	0	0	4.6	1.0004	1	28.0	1.4480	2.10	73.8	70.067	ON
158	0	0.7	1.8	95.7	GH012705 5	3/29/2021	146	72	7.0	1650	0	5	77	9	1	5	8	10.0	0	2.50	0	0	2.7	1.0007	1	21.6	1.3353	1.78	95.7	85.541	ON
159	0	0.4	1.7	113.1	GH012703 1	3/29/2021	141	72	7.0	1650	0	5	77	9	1	5	3	10.0	0	6.50	2	0	1.9	1.0002	1	18.3	1.2625	1.59	113.1	101.447	ON
160	0	0.8	1.6	69.6	GH012703 1	3/29/2021	142	72	7.0	1650	0	3	77	9	1	5	7	10.0	0	8.00	2	0	5.1	1.0004	1	29.7	1.4735	2.17	69.6	67.848	ON
161	0	0.35	1.4	80.85	GH020180 3	3/22/2021	142	72	7.0	1100	1	7	77	2	10	30	5	0.0	0	8.00	1	0	3.8	1.0004	1	25.6	1.4084	1.98	80.9	74.361	ON
162	0	0.7	1.3	55.2	GH030152 2	3/8/2021	64	42	3.0	1650	0	5	77	2	10	60	7	15.0	0	6.50	0	0	8.2	1.0008	1	37.5	1.5743	2.48	55.2	62.337	ON
163	0	0.1	1.1	78	GH010150 5	3/4/2021	55	44	7.0	1650	0	7	77	9	1	5	1	1.0	0	6.50	2	0	4.1	1.0004	1	26.5	1.4240	2.03	78.0	72.532	ON
164	0	0.1	1.1	78	GH010150 1	3/4/2021	57	44	7.0	1650	0	7	77	9	1	5	1	1.0	0	2.50	1	0	4.1	1.0010	1	26.5	1.4242	2.03	78.0	72.635	ON
165	0	0.7	1.1	34.8	GH012703 1	3/29/2021	148	72	7.0	1650	0	1	77	9	10	5	4	10.0	0	2.50	2	0	20.5	1.0050	1	59.5	1.7765	3.16	34.8	55.735	ON
166	0	0.6	1	34.8	GH012703 1	3/29/2021	153	72	7.0	1650	0	1	77	9	1	5	4	10.0	0	2.50	2	0	20.5	1.0050	1	59.5	1.7765	3.16	34.8	55.735	ON
167	0	0.1	0.9	73.6	GH020012 1	4/12/2021	173	63	3.0	1650	0	7	77	8	1	5	3	15.0	0	2.50	1	0	4.6	1.0011	1	28.1	1.4495	2.10	73.6	70.086	ON
168	0	0.4	0.8	36.8	GH010012 1	4/12/2021	172	63	3.0	1650	0	5	77	8	4	5	1	15.0	0	6.50	1	0	18.3	1.0017	1	56.2	1.7508	3.07	36.8	55.959	ON
169	0	0	0.6	52.2	GH010007 6	4/8/2021	162	60	10.0	1650	0	5	77	8	1	5	8	10.0	0	2.50	1	0	9.1	1.0022	1	39.6	1.5992	2.56	52.2	61.934	ON
170	0	0.4	0.6	17.4	GH060018 9	4/22/2012	185	52	3.0	1650	0	1	77	8	1	5	6	10.0	0	8.00	2	1	82.1	1.0062	1	118.9	2.0780	4.32	17.4	-31.494	ON
171	0	0.2	0.4	17.4	GH020034 4	3/8/2021	82	66	9.0	1650	0	1	77	3	3	5	7	10.0	0	8.00	1	7	82.1	1.0147	1	118.9	2.0817	4.33	17.4	-25.633	ON
172	0	0.1	0.4	27.6	GH040001 1	3/30/2021	150	59	9.0	1650	1	1	77	3	20	5	5	15.0	0	2.50	0	0	32.6	1.0079	1	75.0	1.8784	3.53	27.6	44.941	ON
173		0	0.35	29.05	GH01019 -15	1/18/2021	11	50	7.0	1650	0	7	77	9	1	5	4	6.0	0	8.00	2	7	29.4	1.0022	1	71.2	1.8537	3.44	29.1	45.651	ON
174	2.7	3.3	4.5	104.4	GH050026 1	2/24/2021	26	62	9.0	1400	1	7	77	7	10	30	3	10.0	100	6.50	2	0	0.0	1.0000	0	19.8	1.2972	1.68	104.4	93.133	OFF
175	0	5.6	6	38.8	GH020038 0	3/12/2021	98	58	6.0	700	3	5	77	2	1	70	1	20.0	60	1.00	1	7	0.0	1.0000	0	53.3	1.7271	2.98	38.8	56.544	OFF
176	6.6	7.3	10.1	243.6	GH050026 1	2/24/2021	25	61	9.0	1400	1	7	77	4	100	30	3	10.0	50	8.00	2	0	0.0	1.0000	0	8.5	0.9292	0.86	243.6	256.060	OFF
177	0	3.2	4.5	126.1	GH010038 1	3/12/2021	97	58	6.0	700	3	4	77	1	3	40	8	20.0	50	1.00	1	0	0.0	1.0000	0	16.4	1.2152	1.48	126.1	114.821	OFF
178	1.1	1.6	1.9	25.5	GH050026 1	2/24/2021	27	62	9.0	1100	1	3	77	5	1	30	5	8.0	50	2.50	1	0	0.0	1.0000	0	81.2	1.9094	3.65	25.5	33.468	OFF
179	0	0.8	1.6	68	GH060026 1	2/24/2021	28	62	9.0	1100	1	3	77	5	1	30	5	8.0	50	2.50	1	0	0.0	1.0000	0	30.4	1.4834	2.20	68.0	66.991	OFF
180	0	0.7	1.6	82.8	GH010005 3	4/5/2021	154	63	12.0	1650	1	6	77	7	2	50	2	15.0	50	6.50	0	0	0.0	1.0000	0	25.0	1.3979	1.95	82.8	75.607	OFF
181	0	4.1	6.2	193.2	GH030161 1	3/12/2021	113	60	7.0	700	3	7	77	4	1000	40	3	15.0	40	1.00	1	0	0.0	1.0000	0	10.7	1.0299	1.06	193.2	193.601	OFF
182	0	3	3.9	78.3	GH010025 1	4/28/2021	192	74	9.0	1100	1	4	77	9	2	40	6	10.0	40	6.50	0	0	0.0	1.0000	0	26.4	1.4221	2.02	78.3	72.654	OFF
183	0	1.05	3	97.5	GH010159 5	3/9/2021	86	51	7.0	1100	2	5	35	7	1	0	1	15.0	40	1.00	1	0	0.0	1.0000	0	21.2	1.3269	1.76	97.5	87.001	OFF
184	0	1.5	1.9	36.8	GH020159 5	3/9/2021	89	51	7.0	1100	2	7	77	2	1	30	3	15.0	35	1.25	1	0	0.0	1.0000	0	56.2	1.7501	3.06	36.8	55.216	OFF
185	0	10	11.4	70	GH120187 3	3/24/2021	144	72	7.0	1650	0	5	50	6	1	15	5	0.0	30	2.50	1	0	0.0	1.0000	0	29.6	1.4708	2.16	70.0	67.967	OFF
186	0	6.8	9.2	180	GH030160 3	3/12/2021	109	60	7.0	700	3	5	60	9	1	0	3	15.0	30	1.00	1	0	0.0	1.0000	0	11.5	1.0606	1.12	180.0	177.410	OFF
187	0	3.2	6.9	296	GH030159 1	3/9/2021	92	51	7.0	1100	2	5	60	2	8	10	1	20.0	30	1.25	1	0	0.0	1.0000	0	7.0	0.8446	0.71	296.0	320.256	OFF
188	4	5.5	6.8	119.6	GH012703 1	3/29/2021	150	72	7.0	1650	0	5	77	7	1	15	8	15.0	30	2.50	1	0	0.0	1.0000	0	17.3	1.2382	1.53	119.6	108.002	OFF
189	0	4.6	5.6	65	GH020038 1	3/12/2021	99	51	7.0	700	3	5	50	2	1	15	2	15.0	30	1.00	1	0	0.0	1.0000	0	31.8	1.5030	2.26	65.0	65.641	OFF
190	0	1.8	4.1	161	GH010004 0	4/5/2021	153	63	12.0	1650	0	5	60	7	1	5	3	10.0	25	2.50	0	0	0.0	1.0000	0	12.9	1.1091	1.23	161.0	154.497	OFF
191	0	7.6	11.2	144	GH020024 8	4/28/2021	194	74	9.0	1100	1	1	30	4	3	5	4	10.0	20	6.50	0	0	0.0	1.0000	0	14.4	1.1575	1.34	144.0	134.648	OFF
192	0	4.5	5.5	92	GH030038 5	3/12/2021	101	58	6.0	700	3	3	77	9	1	10	5	15.0	20	1.00	1	0	0.0	1.0000	0	22.5	1.3521	1.83	92.0	82.449	OFF
193	0	2.4	3.1	64.4	GH030038 4	3/12/2021	100	51	7.0	700	3	3	77	9	1	10	7	15.0	20	1.00	1	0	0.0	1.0000	0	32.1	1.5070	2.27	64.4	65.388	OFF
194	0	1.8	2.8	92	GH030038 6	3/12/2021	103	58	6.0	700	3	3	77	9	1	10	5	15.0	20	1.00	1	0	0.0	1.0000	0	22.5	1.3521	1.83	92.0	82.449	OFF
195	0	1.2	2	73.6	GH030038 5	3/12/2021	102	58	6.0	700	3	3	77	9	1	10	5	15.0	20	1.00	1	0	0.0	1.0000	0	28.1	1.4490	2.10	73.6	69.875	OFF
196	0	3.7	4.5	69.6	GH020003 0	4/5/2021	156	63	12.0	1650	1	5	77	8	20	1	5	10.0	15	2.50	0	0	0.0	1.0000	0	29.7	1.4733	2.17	69.6	67.767	OFF
197	0	1.9	3.4	138	GH030161 1	3/12/2021	112	60	7.0	700	3	3	77	4	300	50	1	15.0	15	1.00	1	0	0.0	1.0000	0	15.0	1.1760	1.38	138.0	127.855	OFF
198	0	1	2	87	GH020029 1	4/28/2021	195	74	9.0	1100	1	5	77	7	1	5	2	10.0	15	2.50	0	0	0.0	1.0000	0	23.8	1.3764	1.89	87.0	78.603	OFF
199	0	7.7	8.1	34.8	GH020032 2	4/30/2021	204	65	4.0	1650	0	1	77	9	1	5	1	10.0	10	8.00	1	0	0.0	1.0000	0	59.5	1.7743	3.15	34.8	53.479	OFF
200	0	0.7	2.6	165.3	GH010161 1	3/12/2021	104	58	6.0	700	3	3	77	6	1	5	5	10.0	10	1.00	1	0	0.0	1.0000	0	12.5	1.0976	1.20	165.3	159.629	OFF
201	0	2	2.6	52.2	GH010031 1	4/30/2021	200	65	4.0	1650	0	7	77	6	1	5	1	10.0	10	2.50	1	0	0.0	1.0000	0	39.6	1.5982	2.55	52.2	61.247	OFF
202	0	0.6	2.1	138	GH030161 1	3/12/2021	114	60	7.0	700	3	7	77	4	400	30	5	15.0	10	1.00	1	0	0.0	1.0000	0	15.0	1.1760	1.38	138.0	127.855	OFF
203	0	0.9	1.8	63	GH020024 8	4/28/2021	193	74	9.0	1100	1	1	60	4	3	5	4	10.0	10	6.50	0	0	0.0	1.0000	0	32.9	1.5166	2.30	63.0	64.816	OFF
204	0	1.4	1.7	26.1	GH050020 5	4/26/2021	191	62	10.0	1100	1	7	77	6	1	5	3	10.0	10	8.00	0	0	0.0	1.0000	0	79.3	1.8993	3.61	26.1	35.786	OFF
205	0	0.6	1.4	65.6	GH010031 1	4/30/2021	201	65	4.0	1650	0	5	77	9	1	5	7	5.0	10	2.50	1	1	0.0	1.0000	0	31.5	1.4990	2.25	65.6	65.901	OFF
206	0	0.6	1	34.8	GH022716 1	4/30/2021	202	65	4.0	1650	0	1	77	9	1	5	4	10.0	10	8.00	1	0	0.0	1.0000	0	59.5	1.7743	3.15	34.8	53.479	OFF
207	0	2	4.2	191.4	GH030160 1	3/12/2021	111	60	7.0	700	3	3	77	6	1	20	5	10.0	5	1.00	1	0	0.0	1.0000	0	10.8	1.0340	1.07	191.4	191.384	OFF
208	0	1.7	2.5	56	GH030020 6	4/26/2021	188	62	10.0	1100	1	1	60	9	1	30	3	10.0	5	8.00	0	0	0.0	1.0000	0	37.0	1.5677	2.46	56.0	62.360	OFF
209	0	1.3	2	60.9	GH010032 7	4/30/2021	203	65	4.0	1650	0	1	77	9	2	5	3	10.0	5	2.50	1	0	0.0	1.0000	0	34.0	1.5313	2.34	60.9	64.012	OFF
210	0	0.7	1.4	67.9	GH020020 1	4/26/2021	187	62	10.0	1100	1	7	77	9	1	5	3	20.0	5	2.50	0	0	0.0	1.0000	0	30.5	1.4840	2.20	67.9	66.944	OFF
211	0	11.1	13	165.3	GH012703 1	3/29/2021	151	72	7.0	1650	0	5	77	9	12	5	3	10.0	0	2.50	1	0	0.0	1.0000	0	12.5	1.0976	1.20	165.3	159.629	OFF
212	0	6.3	9.2	174	GH080035 8	5/5/2021	209	68	4.0	1650	0	1	50	9	1	20	3	10.0	0	8.00	1	0	0.0	1.0000	0	11.9	1.0754	1.16	174.0	170.113	OFF
213	0	6.3	6.7	36.8	GH030160 4	3/12/2021	110	60	7.0	700	3	4	77	2	20	15	8	15.0	0	1.00	1	0	0.0	1.0000	0	56.2	1.7501	3.06	36.8	55.216	OFF
214	0	2.4	6.1	222	GH030159 6	3/9/2021	91	51	7.0	1100	2	1	50	2	50	25	3	10.0	0	1.25	1	7	0.0	1.0000	0	9.3	0.9695	0.94	222.0	229.271	OFF
215	0	4.5	5.8	113.1	GH010159 8	3/9/2021	87	51	7.0	1100	2	1	77	2	20	10	5	10.0	0	1.00	1	0	0.0	1.0000	0	18.3	1.2624	1.59	113.1	101.440	OFF
216	0	5	5.7	60.9	GH020160 0	3/12/2021	106	58	6.0	700	3	3	77	9	1	30	5	10.0	0	1.00	1	0	0.0	1.0000	0	34.0	1.5313	2.34	60.9	64.012	OFF
217	0	3.5	5.4	165.3	GH040159 1	3/9/2021	95	51	7.0	1100	2	7	77	9	40	30	1	10.0	0	1.25	1	0	0.0	1.0000	0	12.5	1.0976	1.20	165.3	159.629	OFF

218	0	2	4.6	226.2	GH020160 0	3/12/2021	105	58	6.0	700	3	3	77	4	100	30	5	10.0	0	1.00	1	0	0.0	1.0000	0	9.1	0.9614	0.92	226.2	234.485	OFF
219	0	3.1	4	78.3	GH040020 1	4/26/2021	189	62	10.0	1100	1	7	77	9	1	5	1	10.0	0	2.50	0	0	0.0	1.0000	0	26.4	1.4221	2.02	78.3	72.654	OFF
220	0	3	3.7	60.9	GH040159 1	3/9/2021	96	51	7.0	1100	2	1	77	9	1	10	4	10.0	0	1.25	1	0	0.0	1.0000	0	34.0	1.5313	2.34	60.9	64.012	OFF
221	0	1.4	3.4	174	GH020160 9	3/12/2021	108	60	7.0	700	3	3	77	4	200	5	1	10.0	0	1.00	1	0	0.0	1.0000	0	11.9	1.0754	1.16	174.0	170.113	OFF
222	0	2.6	3.2	58.2	GH030159 1	3/9/2021	93	51	7.0	1100	2	7	77	4	40	10	1	20.0	0	2.50	1	0	0.0	1.0000	0	35.6	1.5510	2.41	58.2	63.066	OFF
223	0	2	3.2	104.4	GH040159 0	3/9/2021	94	51	7.0	1100	2	7	77	9	30	30	1	10.0	0	1.25	1	7	0.0	1.0000	0	19.8	1.2972	1.68	104.4	93.133	OFF
224	0	2	2.8	69.6	GH020160 3	3/12/2021	107	58	6.0	700	3	3	77	9	40	5	5	10.0	0	1.00	1	0	0.0	1.0000	0	29.7	1.4733	2.17	69.6	67.767	OFF
225	0	1.7	2.3	46.2	GH020003 0	4/5/2021	155	63	12.0	1650	1	1	77	8	20	5	5	0.0	0	2.50	0	0	0.0	1.0000	0	44.8	1.6513	2.73	46.2	59.555	OFF
226	0	1.4	2.2	69.6	GH040020 9	4/26/2021	190	62	10.0	1100	1	7	77	9	1	5	1	10.0	0	8.00	0	0	0.0	1.0000	0	29.7	1.4733	2.17	69.6	67.767	OFF
227	0	0	2.1	121.8	GH060026 1	2/24/2021	29	62	9.0	700	1	1	50	5	1	30	7	8.0	0	2.50	1	0	0.0	1.0000	0	17.0	1.2303	1.51	121.8	110.283	OFF
228	0	1.3	2	64.4	GH030159 4	3/9/2021	90	51	7.0	1100	2	3	77	8	1	5	5	15.0	0	1.25	1	0	0.0	1.0000	0	32.1	1.5070	2.27	64.4	65.388	OFF
229	0	1.5	1.9	34.8	GH022715 2	4/30/2021	199	65	4.0	1650	0	1	77	9	2	4	4	10.0	0	8.00	0	0	0.0	1.0000	0	59.5	1.7743	3.15	34.8	53.479	OFF
230	0	1	1.9	78.3	GH020031 0	4/30/2021	204	65	4.0	1650	0	1	77	9	3	5	5	10.0	0	2.50	1	0	0.0	1.0000	0	26.4	1.4221	2.02	78.3	72.654	OFF
231	0	0.2	1.2	87	GH010159 9	3/9/2021	88	51	7.0	1100	2	7	77	2	1	10	5	10.0	0	1.25	1	7	0.0	1.0000	0	23.8	1.3764	1.89	87.0	78.603	OFF
232	0	0.7	1.1	36.8	GH010003 5	4/5/2021	152	63	12.0	1100	1	5	77	6	1	10	3	15.0	0	2.50	0	0	0.0	1.0000	0	56.2	1.7501	3.06	36.8	55.216	OFF
233	0	0.2	0.7	43.5	GH020004 0	4/5/2021	157	63	12.0	1650	1	5	77	6	1	5	8	10.0	0	6.50	1	0	0.0	1.0000	0	47.6	1.6774	2.81	43.5	58.674	OFF
234	sec	sec	sec	meter	Video time			F	Plane met	0=1650	0=none	1=N	meter per	1= geese	# birds (est.)	Plane (AGL) m	1=N	Bird (mps)	Bird m (AGL)	1 (Away)	0= behind	0 = no	ratio	Ratio	0=off	Fig of Merit @ distance		merit	meter	0=no change	0= same direction
235										1=1400	1=partial	2=NE		2=ducks			2=NE			1.25 (±45	2 =head-on	5= partial (<45 degrees)			1=on					1=mild (direction	1 = left (>30 degree)
236										2=11000	2=mostly	3=E		3=small passerines			3=E			2.5 (±90°	1 = side	7= Yes								2=moderate (dire	2 = right (>30 degre
237										3=700	3=overcas	4= SE		4=mix grackles, blackbirds, cow			4= SE			6.5 (±45° | Direct)									3=strong (reverse	3 =split
238												5=S		5=herons egrets ibis			5=S			8 (Direct)											4=up
239												6= SW		6=raptor			6= SW														5=down
240												7=W		7=ravens crows			7=W														6 = all direction
241												8=NW		8=kildeer			8=NW														
242												9=MIXED		9=unk, 10+vulture																	
243	start - vid	act time- v	end - vid	Dist = sec*mps	**Vid file**	**(date) CST**	**Event No.**	**Temp (F)**	**Wind (mps)**	**[I] (lux)**	**Cloud Cover**	**Plane Direction**	**Plane speed (mps)**	**Species**	**Flock size**	**Plane (AGL)**	**Bird Direction**	**Bird speed (mps)**	**Bird (AGL)**	***[F$_1$]***	**Head-on Flight**	**Sun-Plane Backlit**	***[Ee]***	**SNR**	**ON/OFF PAR46**	***[V$_1$]* or *[PH$_{eye}$]***	***[V$_2$]***	***[V$_3$]***	***[Dpb]* (meter)**	**Intensity - Bird Respone *[Rpb]***	**Diversion Direction**